

# High precision measurements of Deeply Virtual Compton Scattering at small nucleon momentum transfer

CLAS Collaboration meeting  
July 2nd, 2026



Juan Sebastian Alvarado  
Mostafa Hoballah  
Eric Voutier

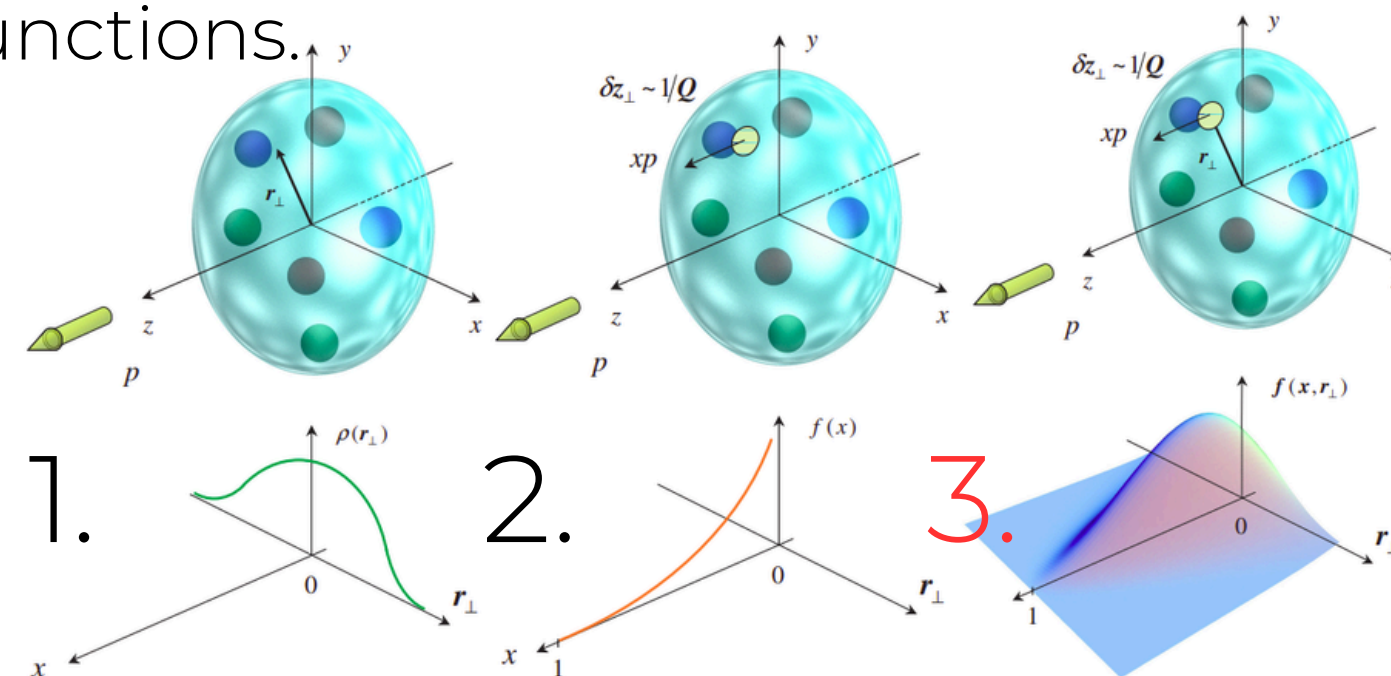


# 1. PROTON GPDS & DVCS

Nucleon internal dynamics is described in terms of structure functions.

They are introduced to describe the partons'

1. Transverse position distribution → FFs
2. Longitudinal momentum distribution → PDFs
3. Transverse position and longitudinal momentum → GPDs
4. Transverse position and transverse momentum → TMDs

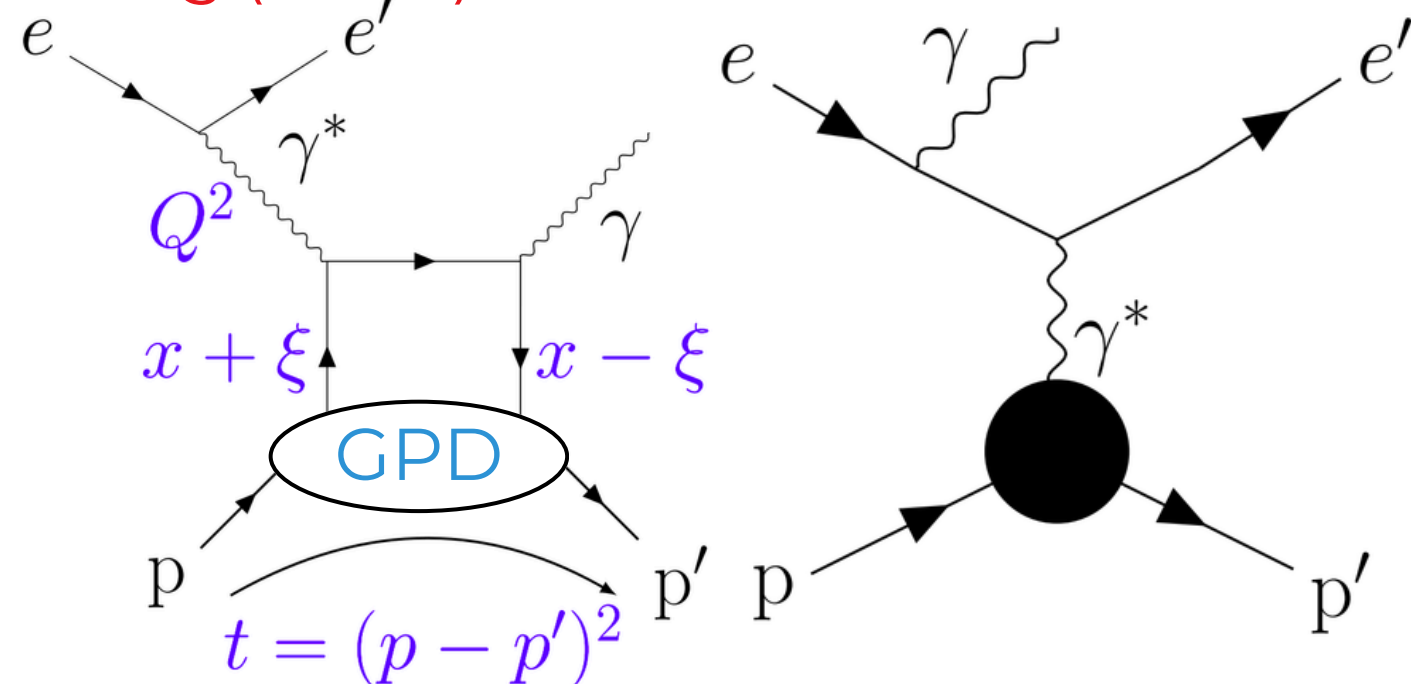


The proton features four chiral-even GPDs  $F = H, E, \tilde{H}, \tilde{E}$

which can be constrained via electro-production of a real photon  $ep \rightarrow epy$

Deeply Virtual Compton Scattering (DVCS)

Bethe-Heitler (BH)



They enter the amplitude through **Compton Form Factors (CFFs)**

$$\mathcal{F}(\xi, t) = \sum_q e_q^2 \left\{ \mathcal{P} \int_{-1}^1 dx F^q(x, \xi, t) \left[ \frac{1}{x - \xi} + \frac{1}{x + \xi} \right] - i\pi [F^q(\xi, \xi, t) - F^q(-\xi, \xi, t)] \right\}$$

In particular, the Beam Spin Asymmetry (BSA) access:

$$\text{BSA} \propto \text{Im} \left\{ F_1 \mathcal{H} + \xi' (F_1 + F_2) \tilde{\mathcal{H}} - \frac{t}{4M_N^2} F_2 \mathcal{E} \right\}$$

# 1. PROTON GPDS & DVCS

Detecting the proton ensures exclusivity of the reaction, but limits the  $|t|$  coverage

$$ep \rightarrow e'p'\gamma \quad t(p' = 0.35 \text{ GeV}/c) \simeq p'^2 = 0.1225 \text{ GeV}^2/c^2$$

## Access to Gravitational Form Factors.

H. Dutrieux *et al.*, Eur. Phys. J. C 81 (2021) 4, 300

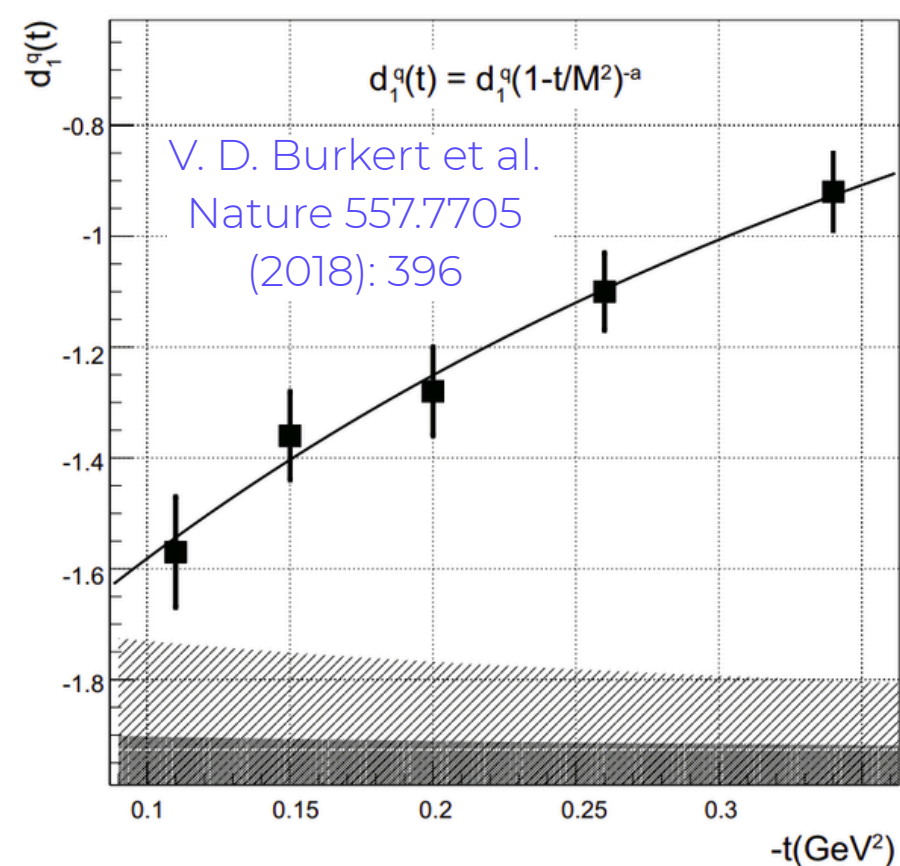
The **D-term** can be constrained through **cross-section** (**Re[CFFs]**) and **BSA** (**Im[CFF]**) measurements

$$D(t) = \Re[\mathcal{H}(\xi, t)] - \frac{1}{\pi} \int_0^1 d\xi' \Im[\mathcal{H}(\xi', t)] \left( \frac{1}{\xi - \xi'} - \frac{1}{\xi + \xi'} \right)$$

The **pressure distribution** within the nucleon can be accessed through  $d_1(t)$

$$D(t) = \frac{1}{2} \int_{-1}^1 \frac{dz}{1-z} (1-z^2) \left[ d_1(t) C_1^{3/2}(z) + \dots \right]$$

$$d_1(t) \equiv d_1(t=0) f_1(t)$$



## 1. Missing the proton is beneficial

- **Unlocks small  $|t|$  values** inaccessible via proton-detection
  - **Down to  $|t|=0.022 \text{ GeV}^2$**
  - Beneficial for a precise  $t=0$  extrapolation
- Larger statistics can be achieved,

## 2. However,

- There is an increased background
- There is less information to constrain the process

## Contributions to the nucleon total spin.

X. Ji, Phys.Rev.Lett.78,610(1997)

$$\frac{1}{2} \Delta\Sigma + \Delta L = \sum_q \frac{1}{2} \int_{-1}^1 dx x (H^q(x, \xi, t=0) + E^q(x, \xi, t=0))$$

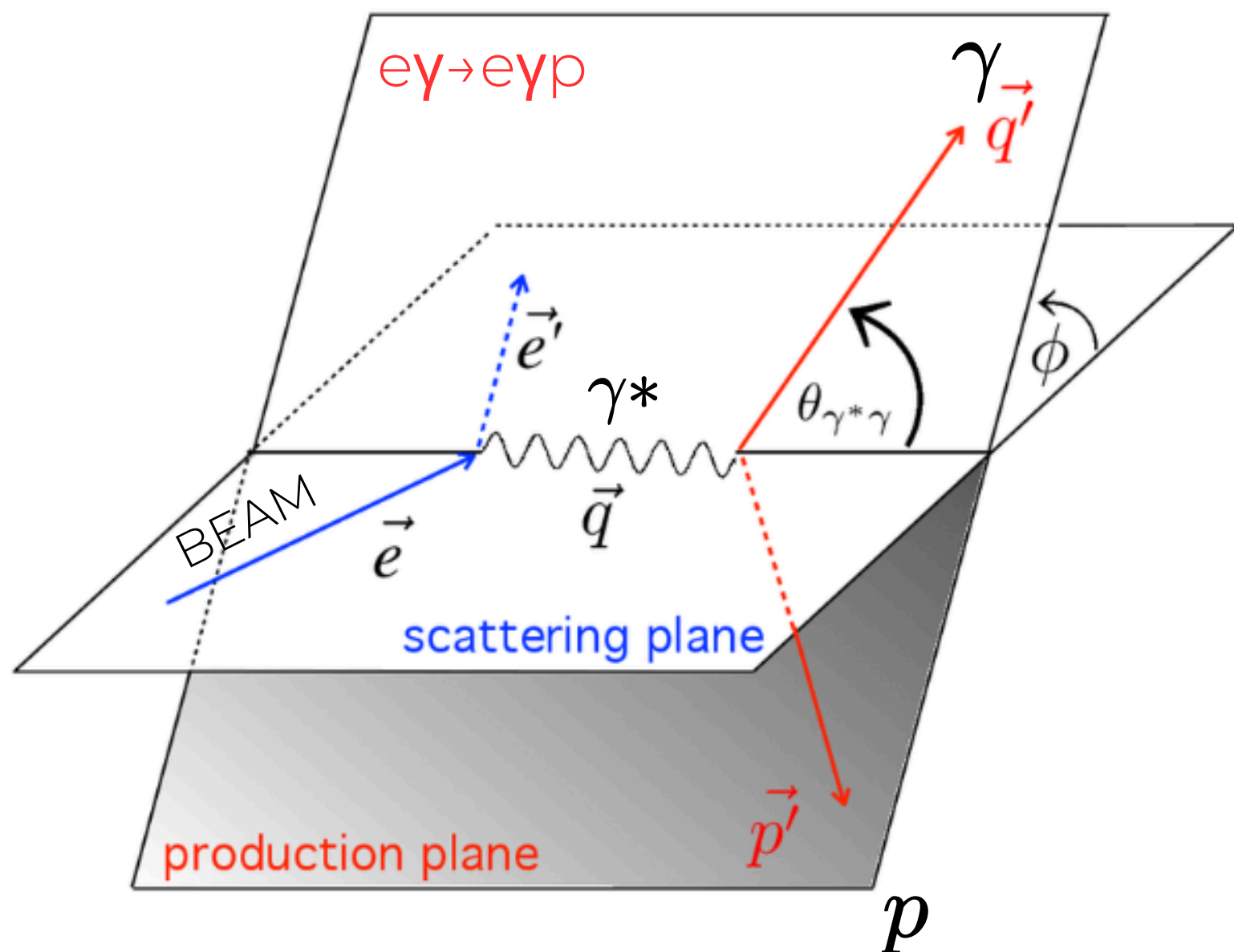
- **Quark spin contribution**
- **Quark's orbital angular momentum**

## 3. Therefore,

- We implement a **ML approach** for channel selection
- Physics results include measurements **with and without** requiring proton detection
- Validation relies on the consistency of both approaches

# 2. DATA SELECTION

- **Fall-2018** RG-A data
  - Polarized electron beam, unpolarized LH<sub>2</sub> target
  - Inbending and outbending data
  - **Pass2** reconstruction



## KINEMATICS

- $W > 2 \text{ GeV}$
- $Q^2 > 1 \text{ GeV}^2$
- $q' > 2 \text{ GeV}/c$
- $e' > 1 \text{ GeV}/c$
- $(p' > 0.3 \text{ GeV}/c)$

## EXCLUSIVITY CUTS

(only if proton detected)

- $\Delta\phi = |\phi(p') - \phi(\gamma)| < 2^\circ$
- $\Delta t = |t(p') - t(\gamma)| < 2 \text{ GeV}^2$
- $P_{\text{miss}} < 1 \text{ GeV}/c$

$\phi(p')$  uses  $\gamma^*$  and  $p'$   
 $\phi(\gamma)$  uses  $\gamma^*$  and  $\gamma$

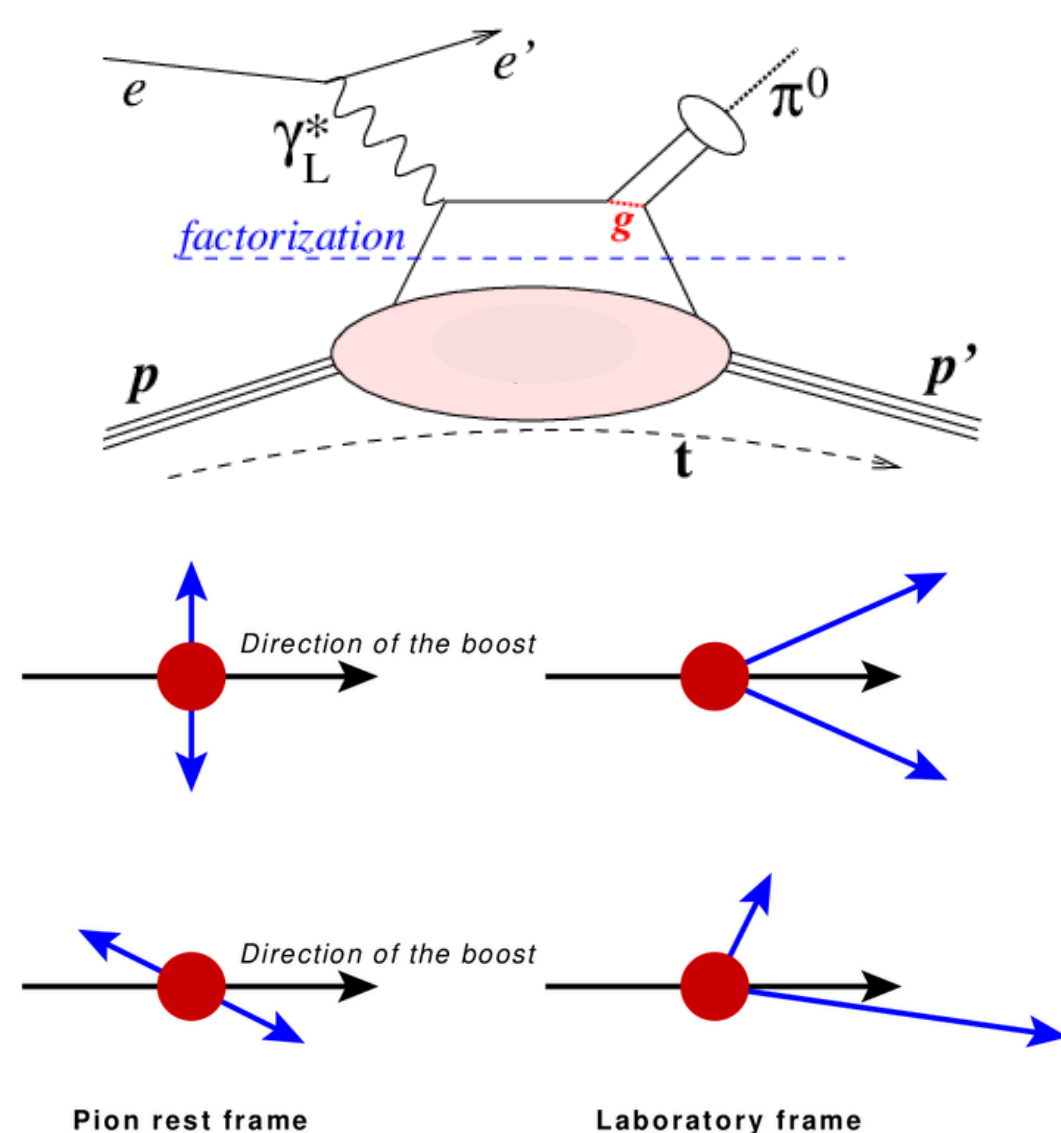
The event is built with the (e,  $\gamma$ , p) set with minimum missing  $ep \rightarrow eyp$  mass

$$t(p') = (p - p')^2$$

$$t(\gamma) = \frac{Q^2 M_p + 2v M_p (v - \sqrt{v^2 + Q^2} \cos \theta_{\gamma^* \gamma})}{\sqrt{v^2 + Q^2} \cos \theta_{\gamma^* \gamma} - v - M_p}$$

# 2. DATA SELECTION

The main background contribution is exclusive  $\pi^0$  production

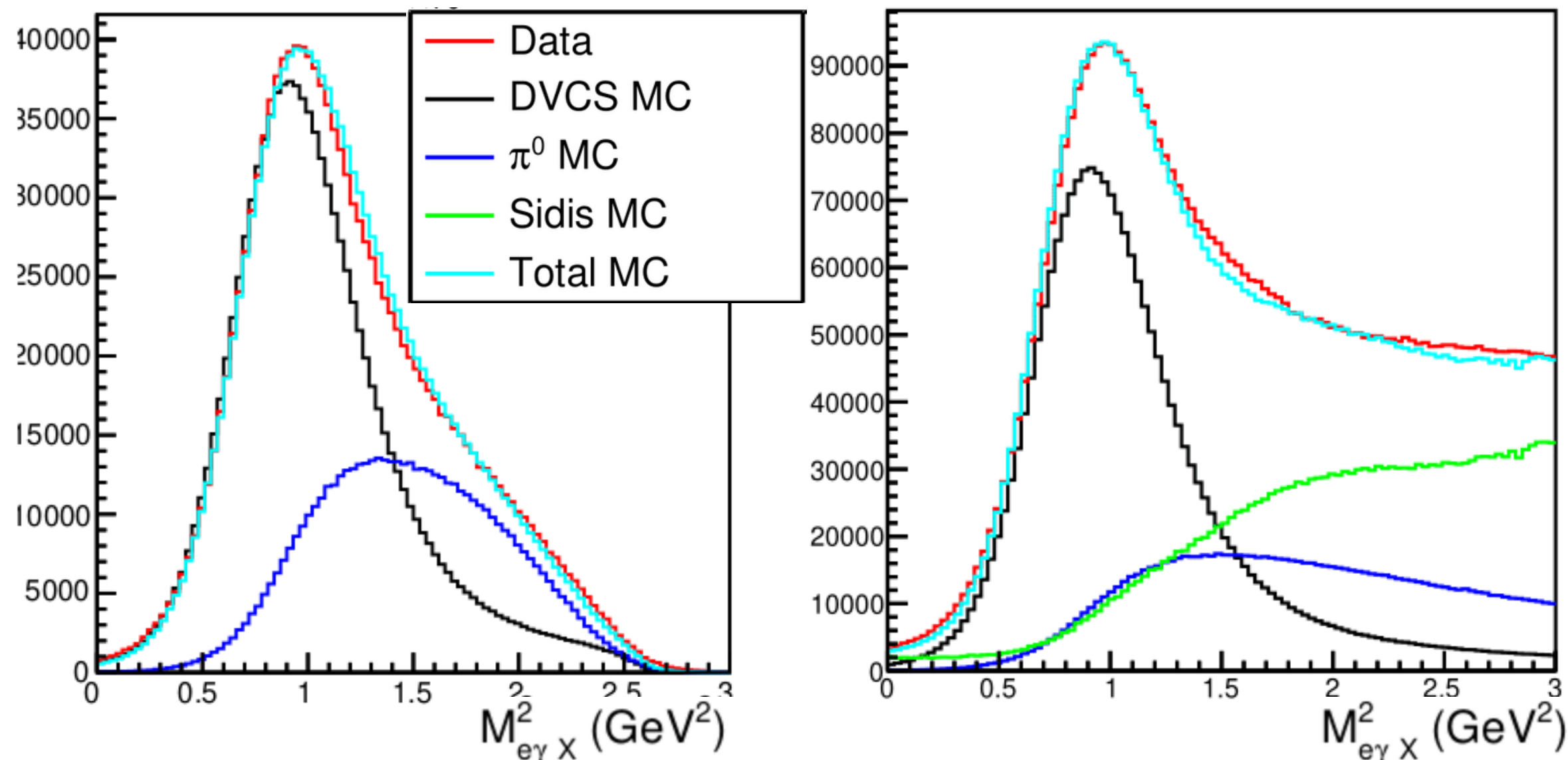


## Missing proton mass distribution

$$M_{e\gamma X}^2 = (e + p - e' - \gamma)^2$$

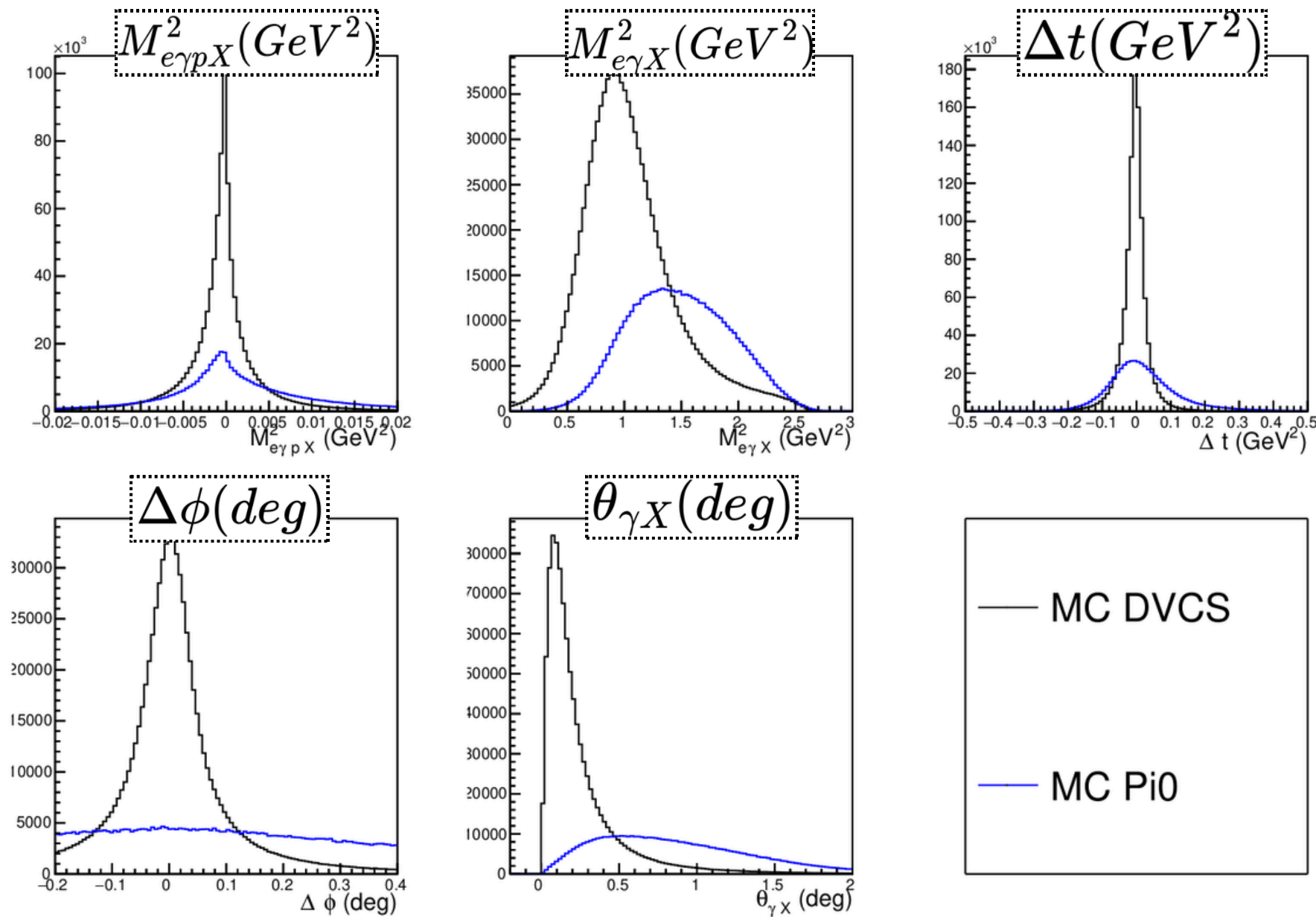
With proton

Without proton



In the case of no proton detection, there is contamination from **inclusive**  $\pi^0$  production from SIDIS

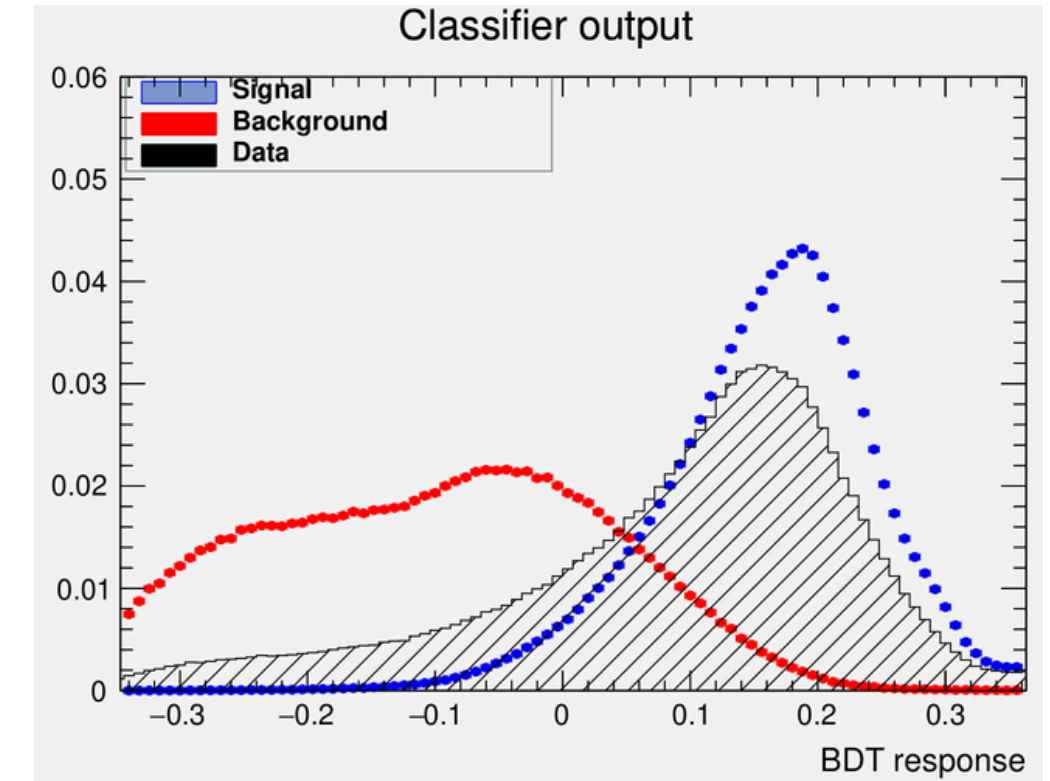
# 3. CHANNEL SELECTION



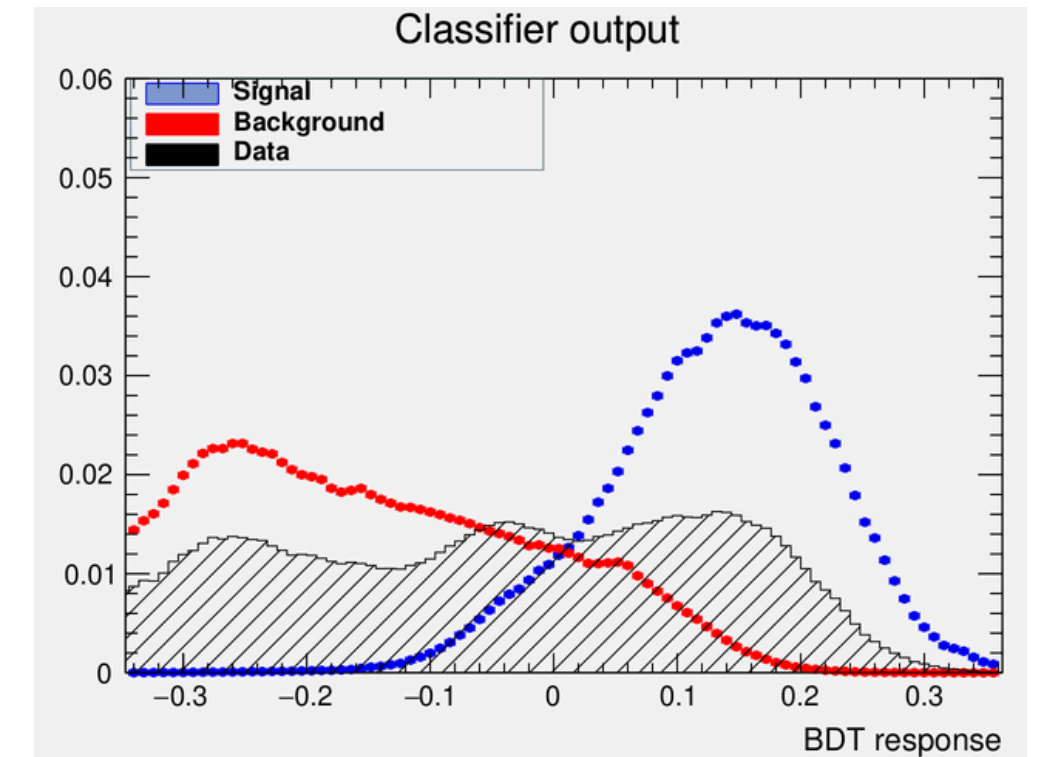
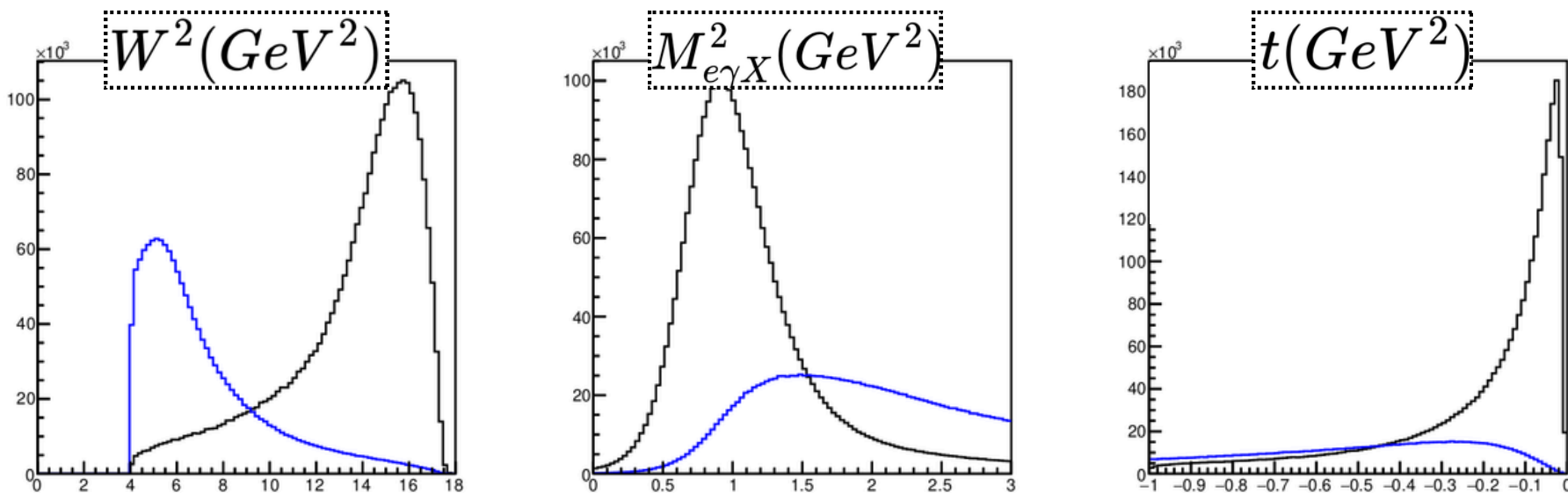
Rather than straight cuts, we optimize data selection with **Boosted Decision Trees**.

With proton

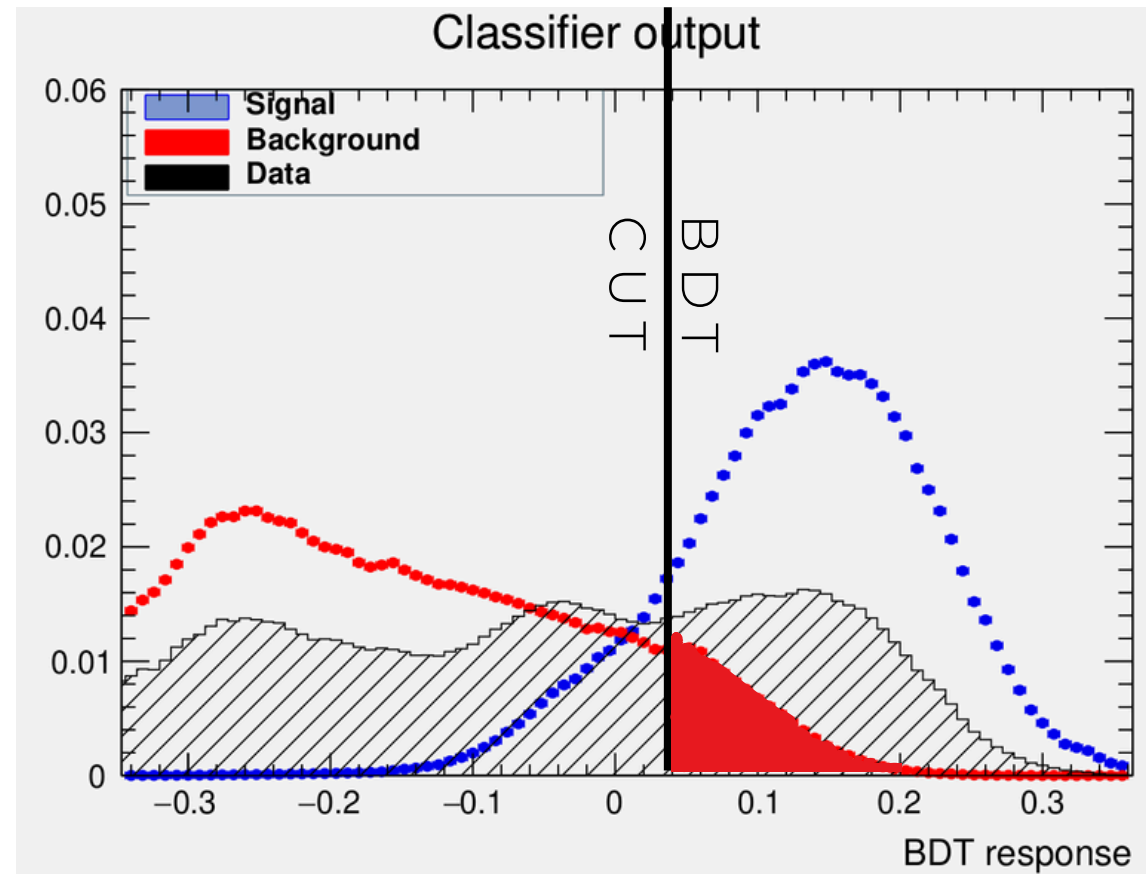
These variables are used to train the BDT model



W/out proton



# 3. CHANNEL SELECTION



The entirety of the background cannot be removed with a BDT

To estimate and remove the residual background, the **1 $\gamma$ /2 $\gamma$  - phase space ratio** is estimated with two methods

$$\frac{(N_{DVMP}^{MC})_{ep \rightarrow ep\gamma}}{(N_{DVMP}^{MC})_{ep \rightarrow ep\gamma\gamma}} = \frac{(N_{DVMP}^{Data})_{ep \rightarrow ep\gamma}}{(N_{DVMP}^{Data})_{ep \rightarrow ep\gamma\gamma}}$$

## METHOD 1

Based on  $ep \rightarrow ep\pi^0 \rightarrow ep\gamma\gamma$  simulations through GEMC,

- $N_{\pi^0 \rightarrow \gamma}^{MC}$ : # of events passing DVCS selection (DVCS contamination)
- $N_{\pi^0 \rightarrow \gamma\gamma}^{MC}$ : # of reconstructed  $\pi^0$  events

•  $N_{\pi^0 \rightarrow \gamma} / N_{\pi^0 \rightarrow \gamma\gamma}$  provides a bin-averaged estimation

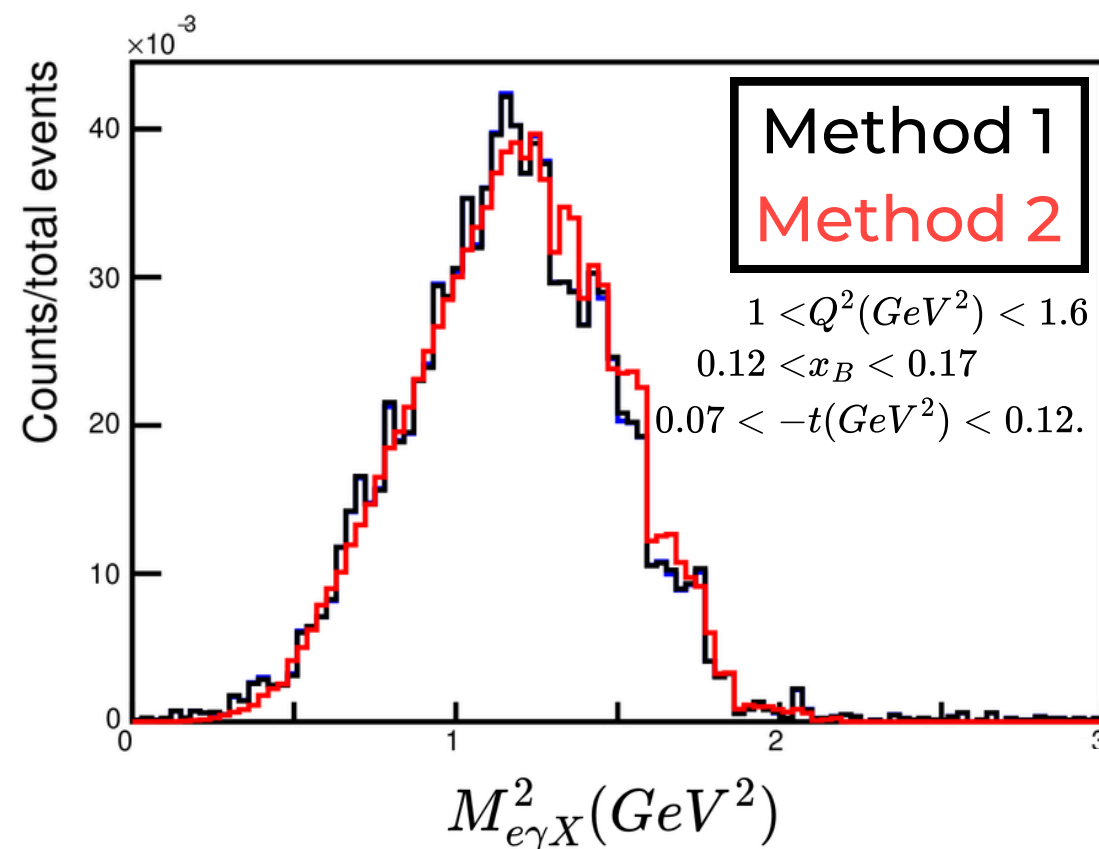
## METHOD 2

We simulate 1500 decays for each experimentally reconstructed  $\pi^0$

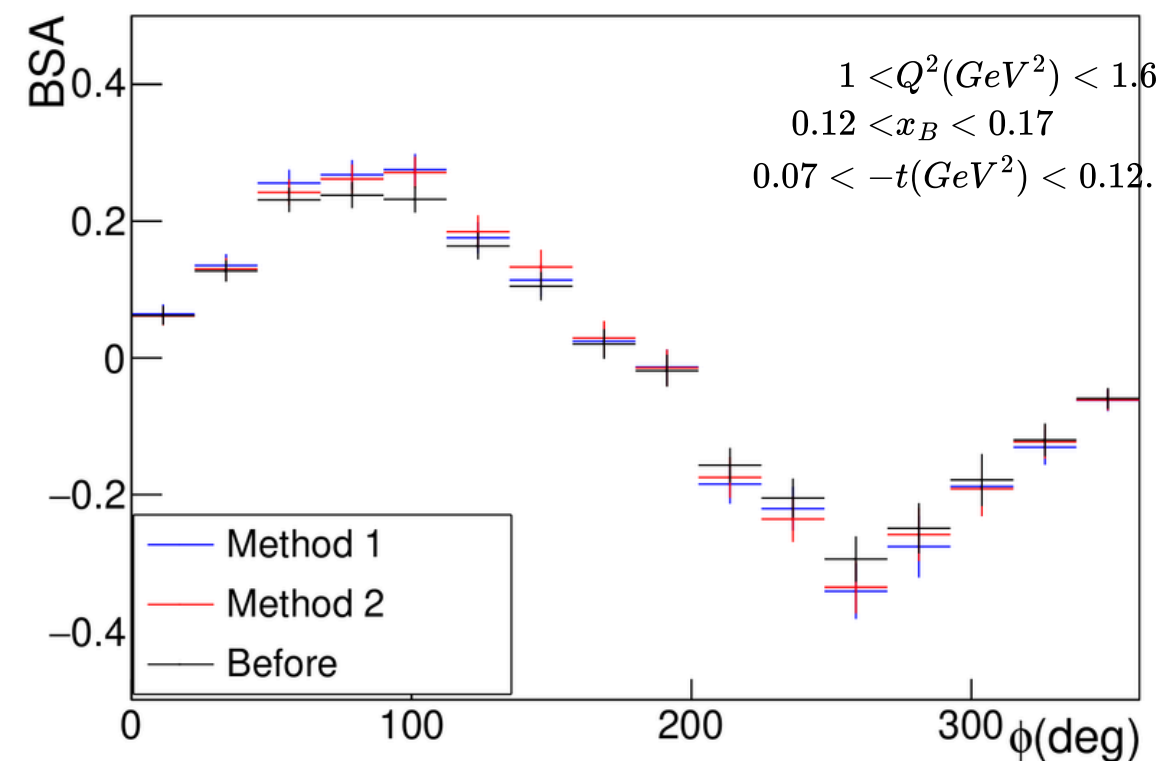
- $N_{\pi^0 \rightarrow \gamma}^{MC}$ : # of detected photons passing DVCS selection
- $N_{\pi^0 \rightarrow \gamma\gamma}^{MC}$ : # of two-photon detected decays
- Photon detection established through acceptance maps
- The total ratio is the sum of individual ratios

•  $N_{\pi^0 \rightarrow \gamma} / N_{\pi^0 \rightarrow \gamma\gamma}$  provides an event-by-event estimation

# 3. CHANNEL SELECTION

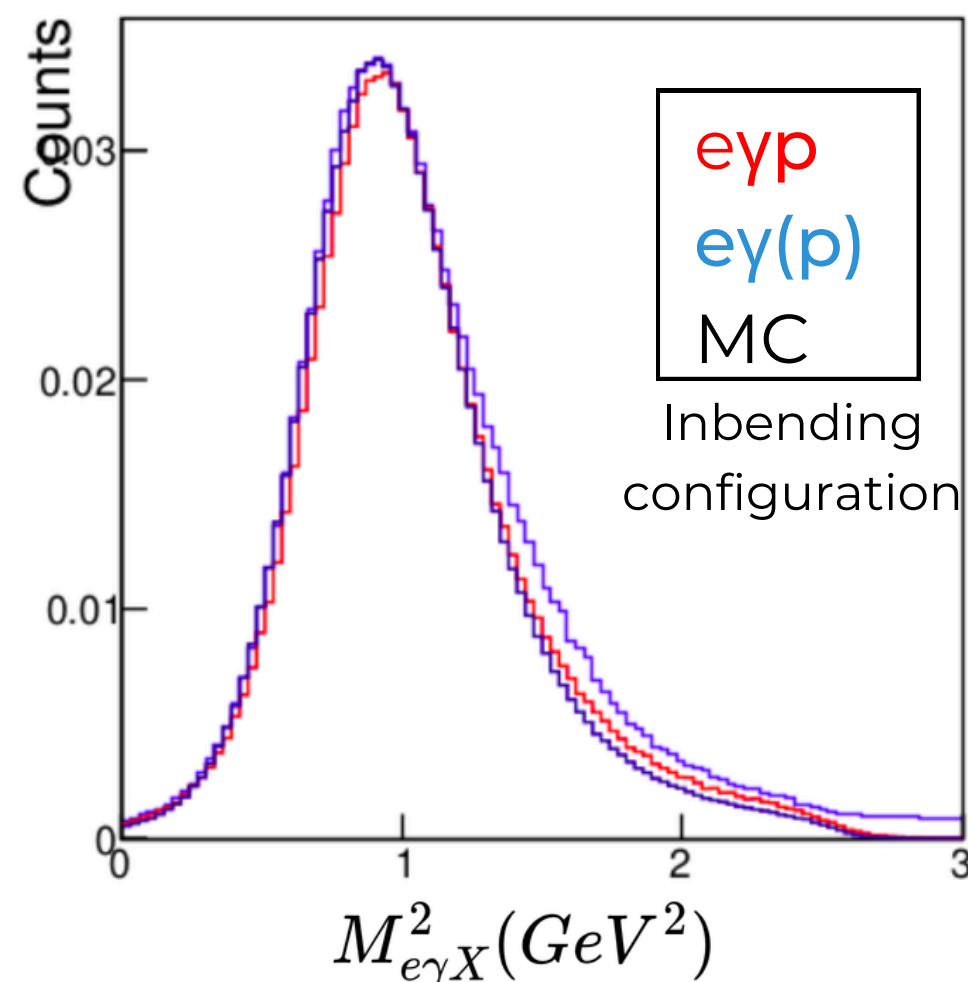


Consistent background estimation from both methods

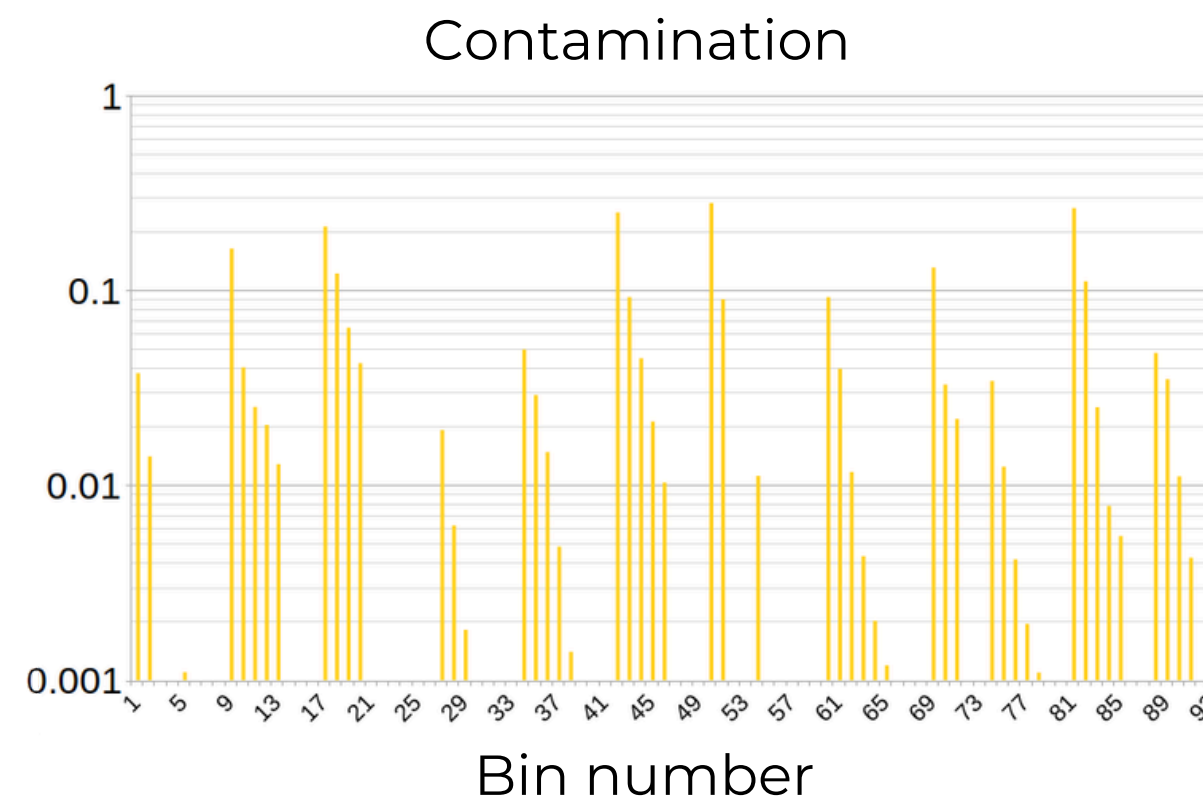


As the background is removed, the asymmetry increases

- Raw measurements are diluted by the  $\pi^0$  asymmetry ( $\sim 5\%$ )



Consistent missing proton mass distributions whether or not the proton is detected

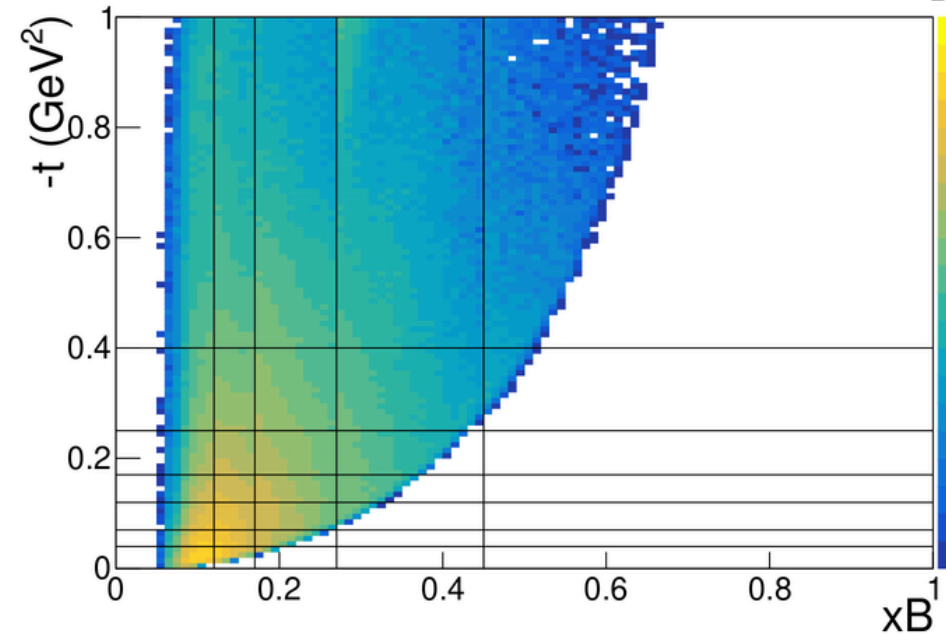
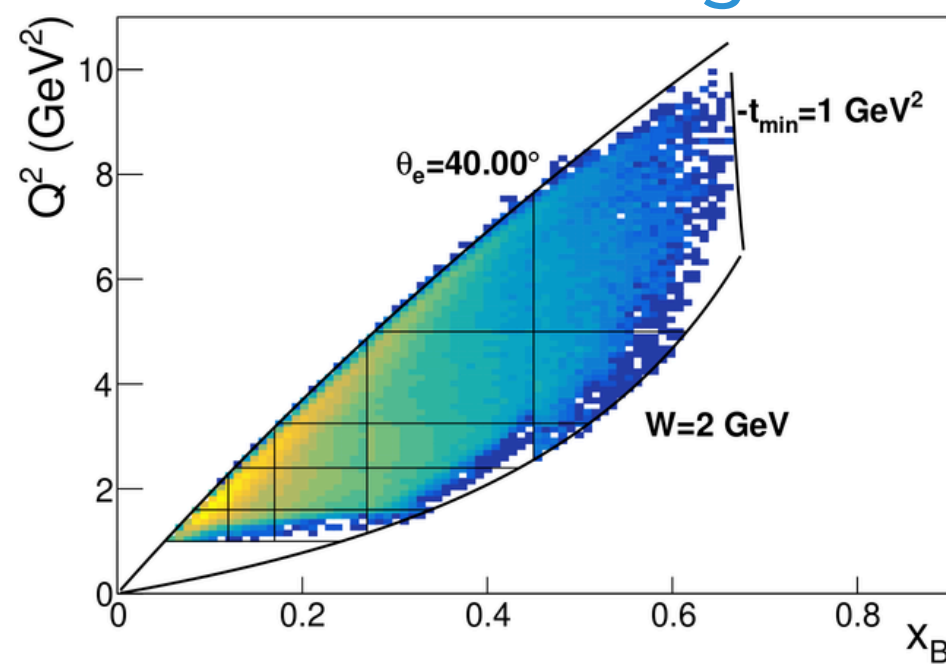


Overall contamination:

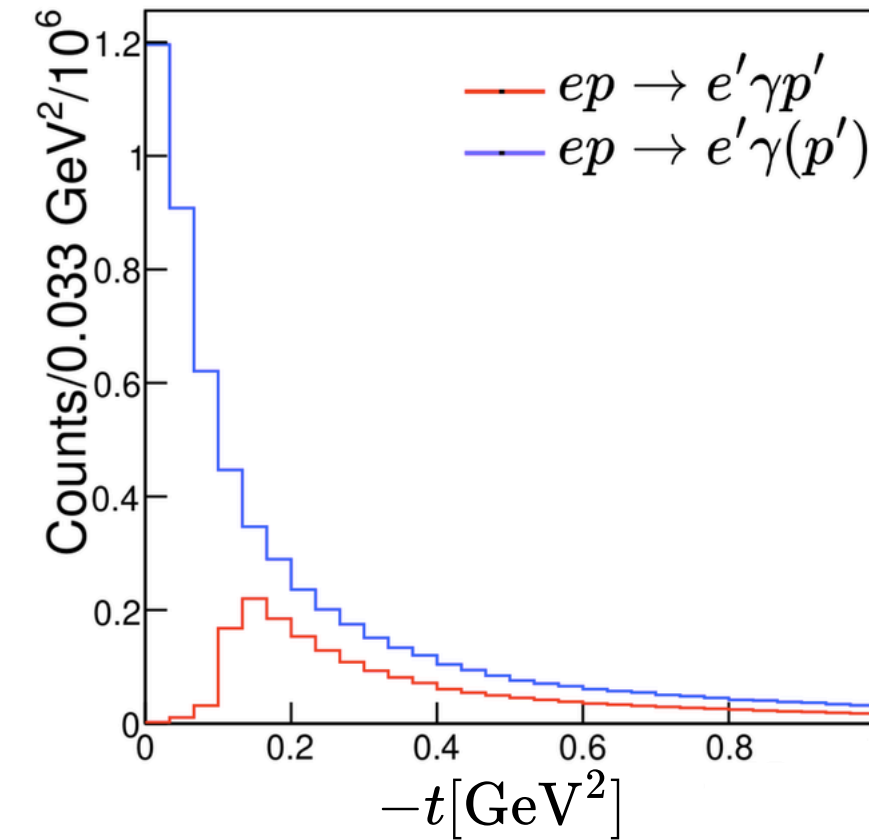
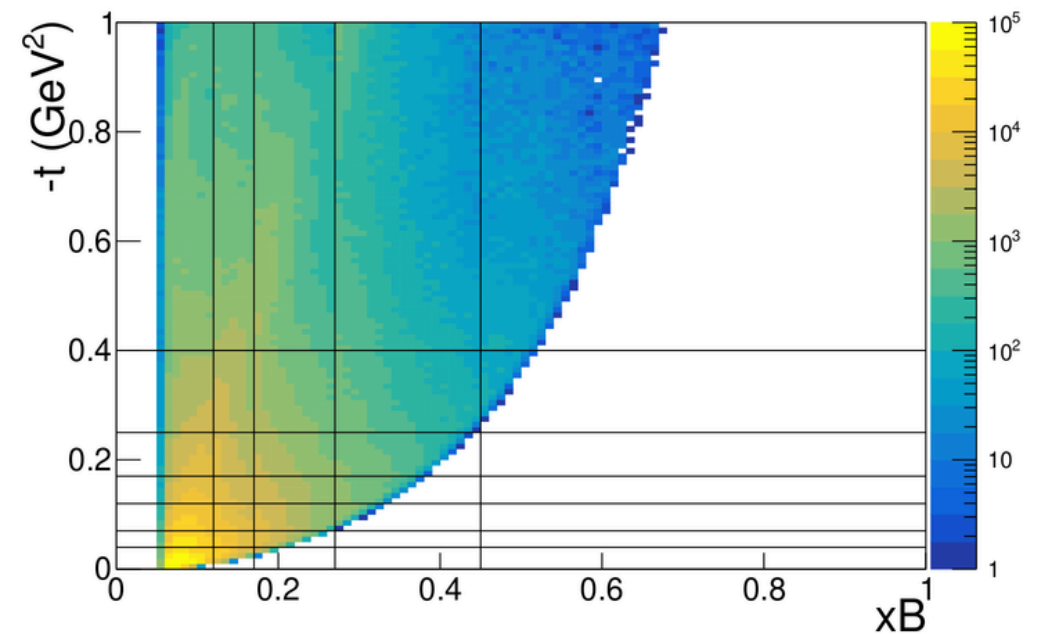
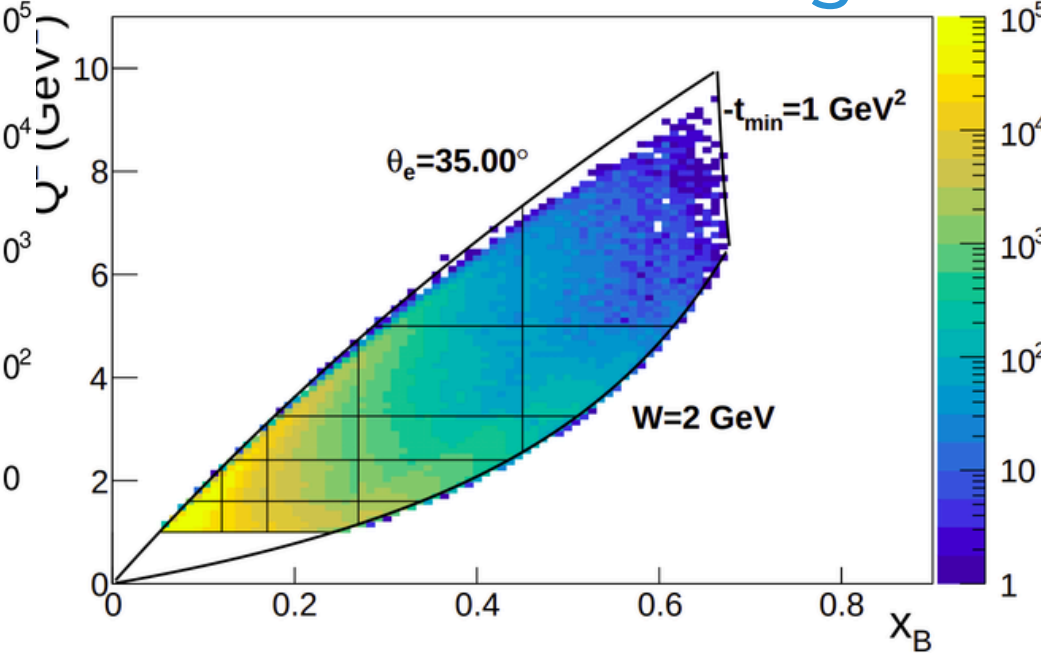
- eyp:  $(6 \pm 3)\%$
- ey(p):  $(4 \pm 1)\%$

# 3. CHANNEL SELECTION

Without proton  
Inbending



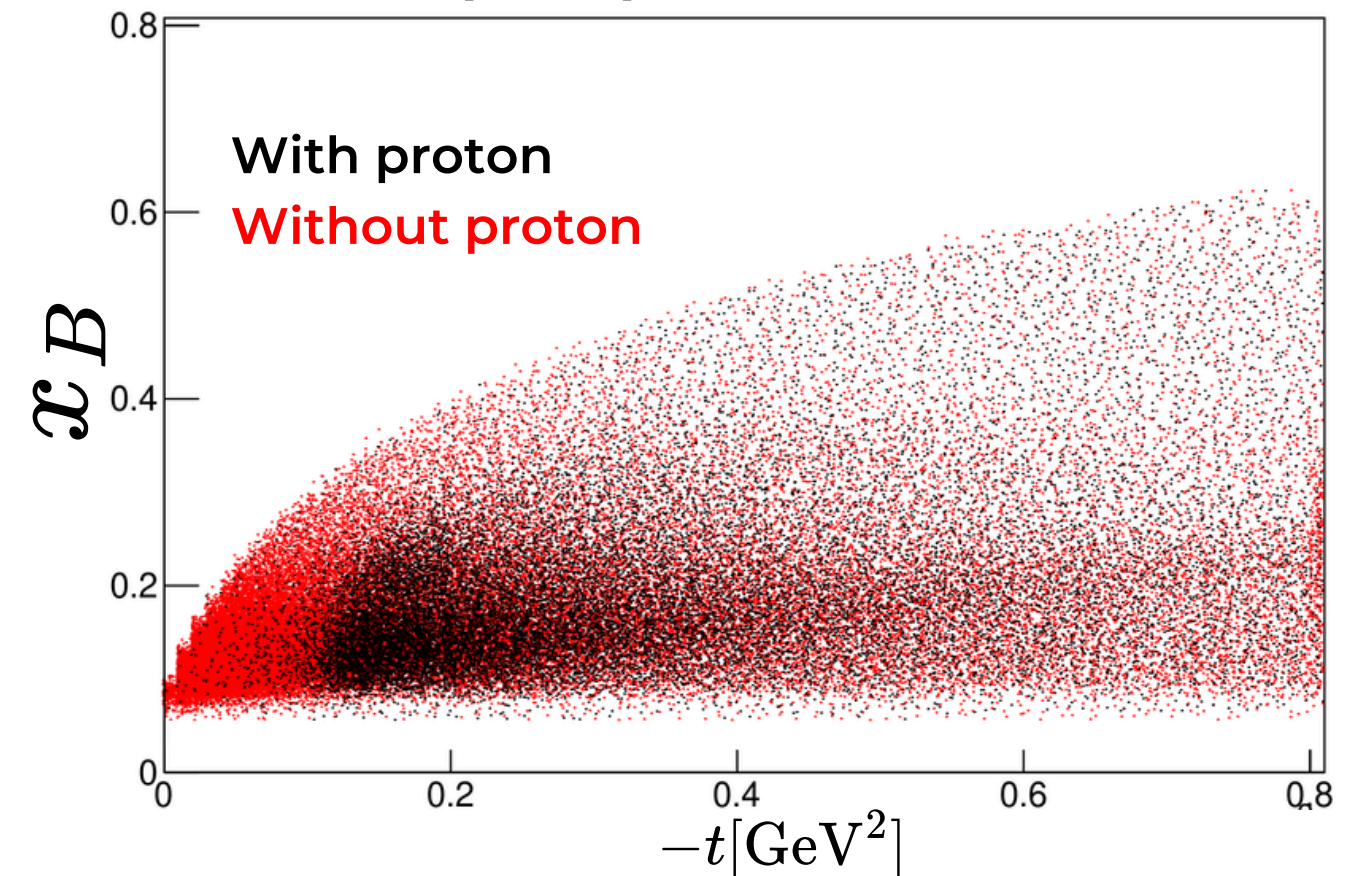
Without proton  
Outbending



When not requiring a proton:

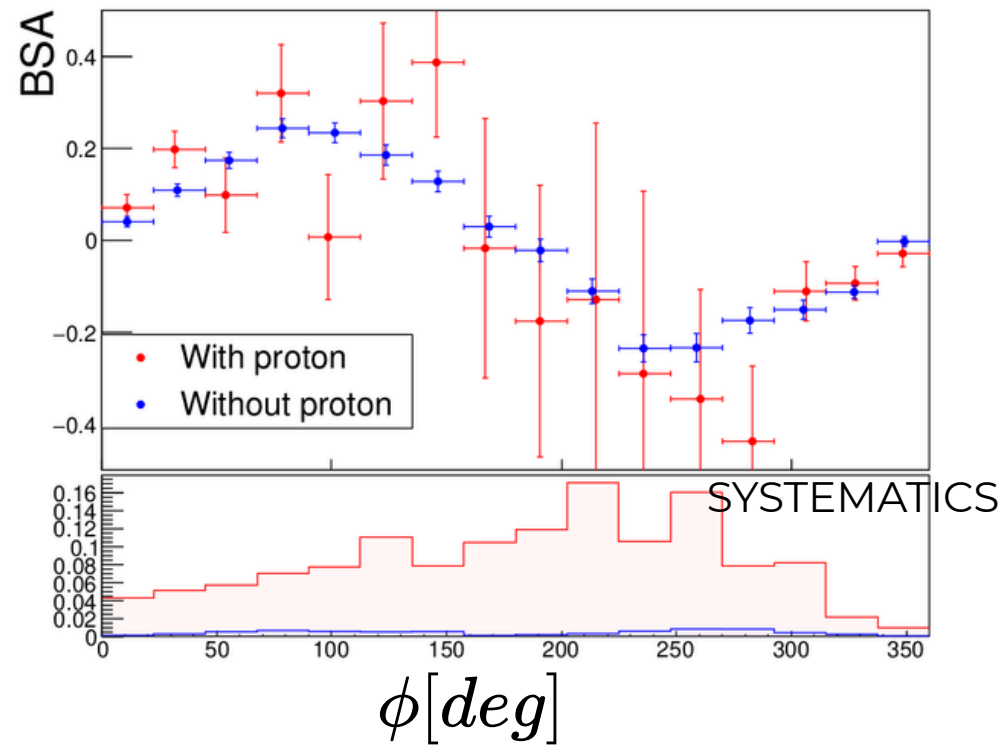
- Increased statistics
- Access to smaller  $-t$  values

- 16 bins on  $(Q^2, x_B)$ , 7 bins in  $t$
- 94 effectively populated bins



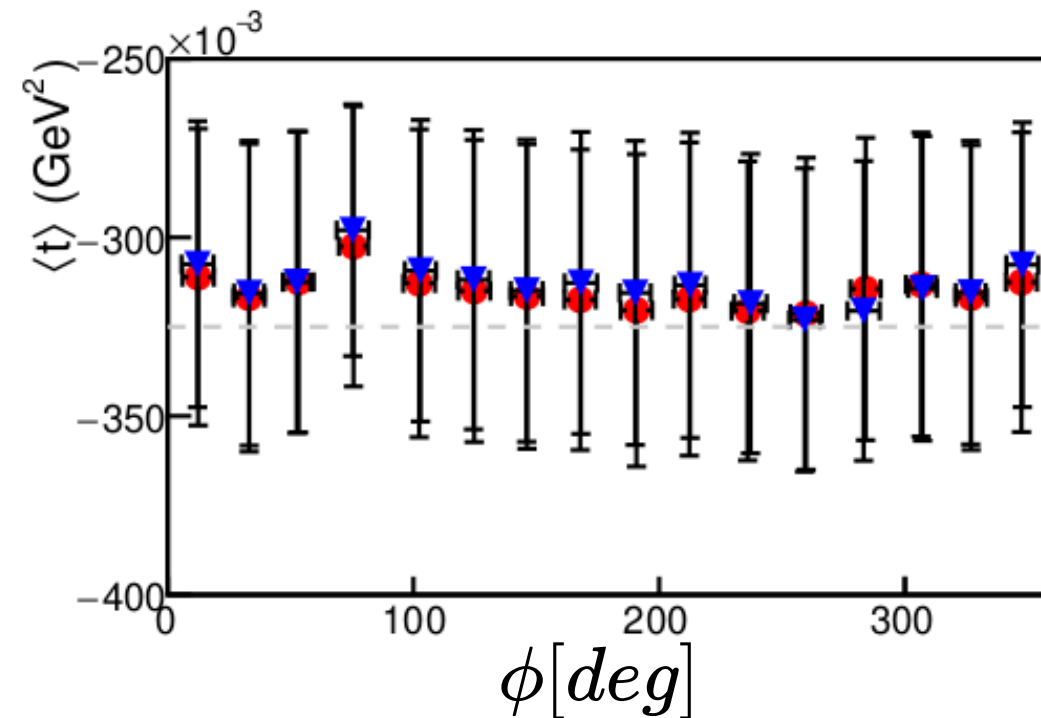
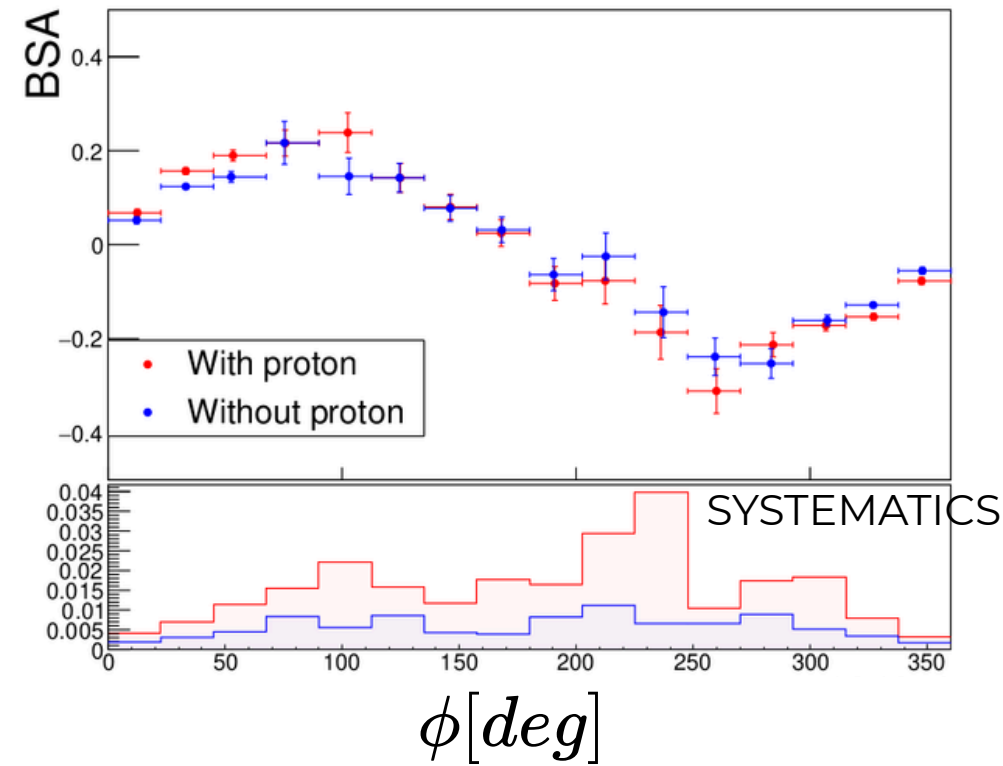
# 4. BEAM SPIN ASYMMETRY

$2.4 < Q^2[\text{GeV}^2] < 3.25, 0.17 < x_B < 0.27$   
 $0.07 < -t[\text{GeV}^2] < 0.12$

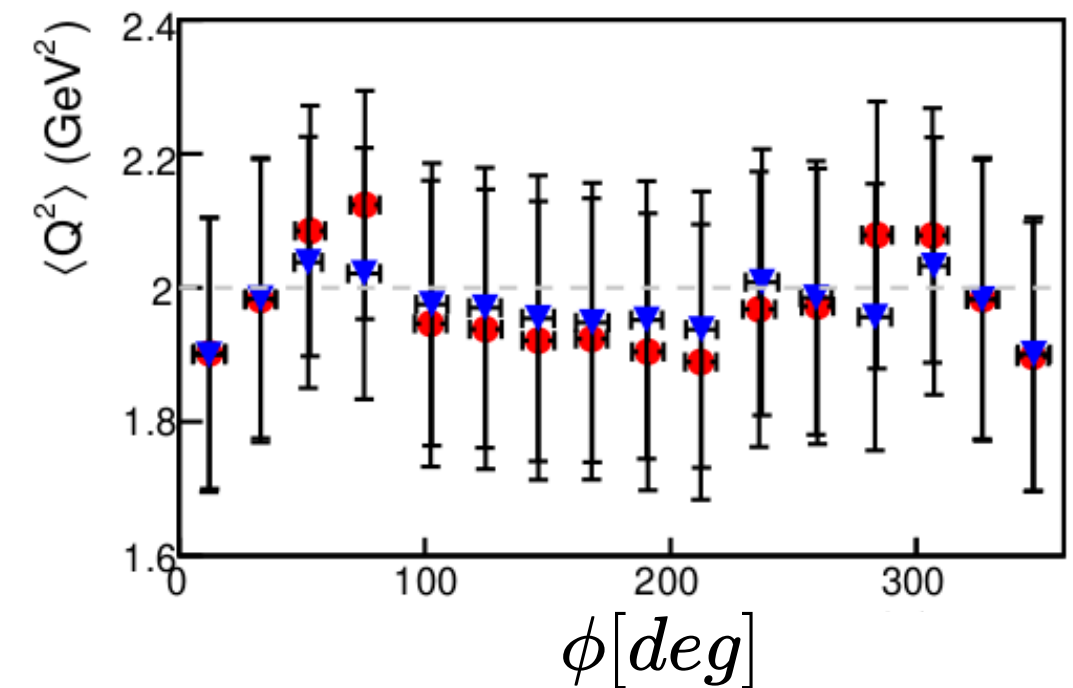
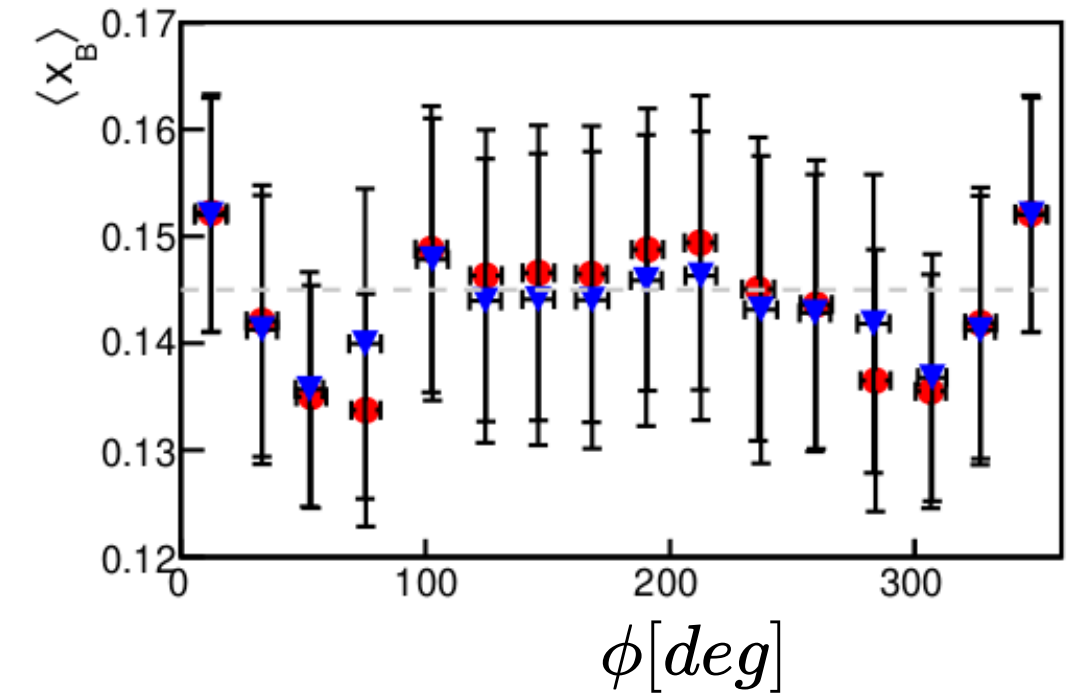


- Small  $-t$  access is granted by not detecting the proton
- Smaller systematic error when not requiring a detected proton

$1.6 < Q^2[\text{GeV}^2] < 2.4, 0.12 < x_B < 0.17$   
 $0.25 < -t[\text{GeV}^2] < 0.4$



In the overlapping region, identical measurements are retrieved



# 4. BEAM SPIN ASYMMETRY: SYSTEMATICS

Systematic uncertainties arise from three main sources:

## Selection cuts / PID Selection / BDT cut

$$\delta A^{cuts} = \frac{\frac{A_{cut}}{\sigma(A_{cut})} - \frac{A}{\sigma(A)}}{\frac{1}{\sigma(A_{cut})} + \frac{1}{\sigma(A)}}$$

$$|\Delta\phi| < 2^\circ \rightarrow |\Delta\phi| < 1.5^\circ$$

$$P_{miss} < 1 \text{ GeV} \rightarrow P_{miss} < 0.8 \text{ GeV.}$$

$$\frac{E_{dep}^{ECIN}}{p_e} > 0.2 - \frac{E_{dep}^{PCAL}}{p_e}$$

$$-13 \text{ cm} < v_z^e < 12 \text{ cm}$$

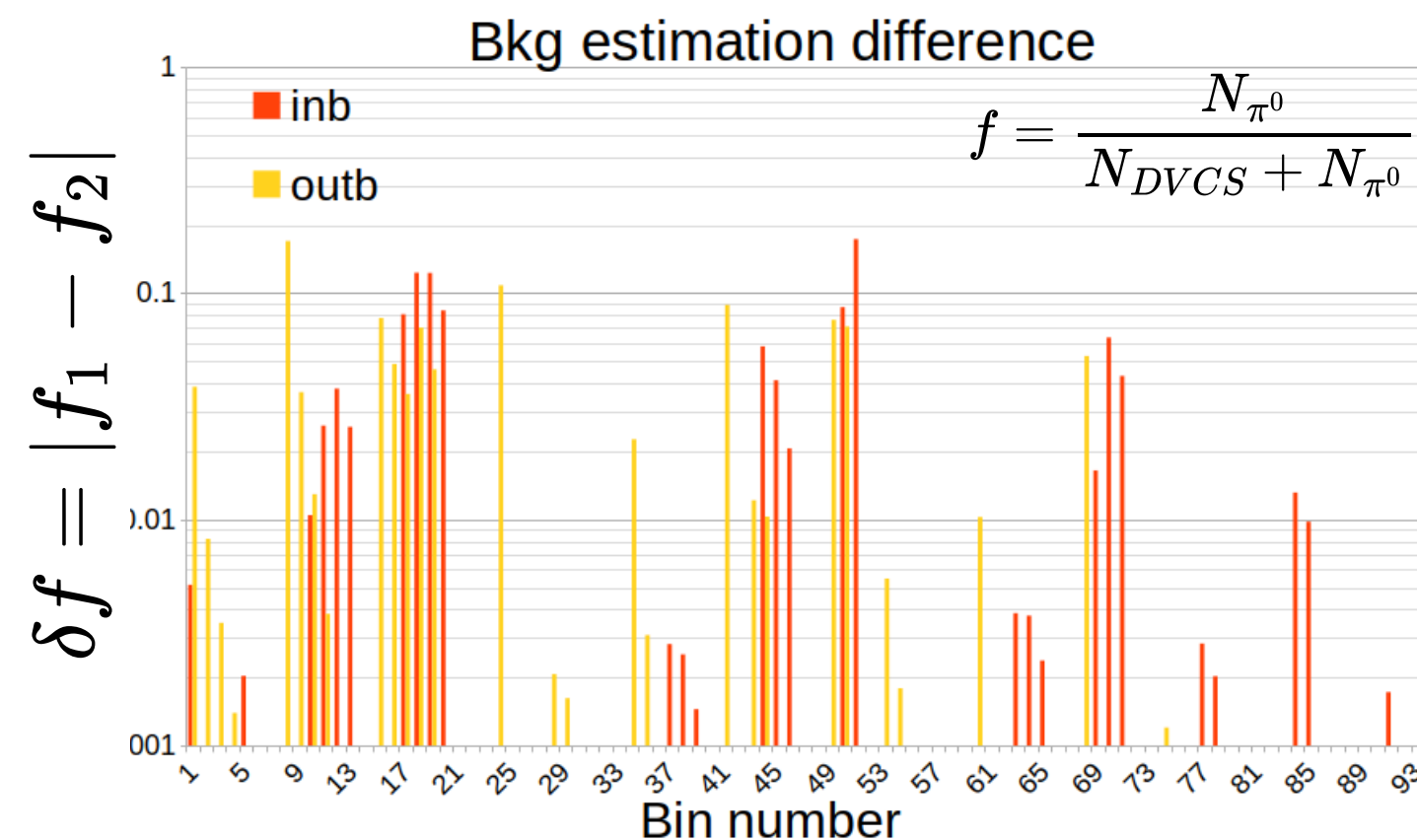
$$|v_z^e - v_z^p| < 20 \text{ cm}$$

$$\text{BDT-Score} \rightarrow \text{BDT-Score} + 0.04$$

BSA was extracted with a modified cut

## Background subtraction.

$$\delta A^{Bkg} = \frac{A^{raw} - A^{\pi^0}}{(1-f)^2} \delta f$$



- The difference between the two estimation methods ( $\delta f = |f_1 - f_2|$ ) yields the systematic error
- Differences are mainly smaller than 10%

## Beam polarization

$$\delta A^{Pol} = A \frac{\delta P}{P}$$

About 2%

# 4. BEAM SPIN ASYMMETRY: SYSTEMATICS

Systematic uncertainties arise from three main sources:

**Selection cuts / PID Selection / BDT cut**

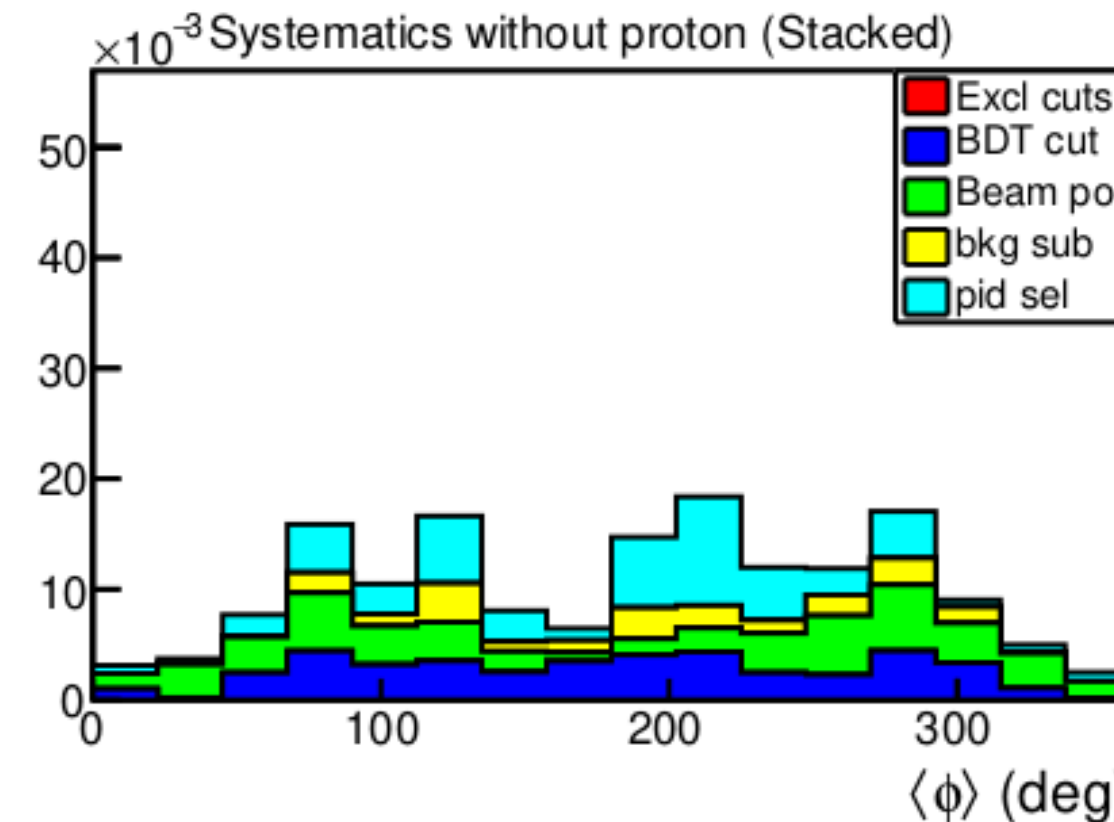
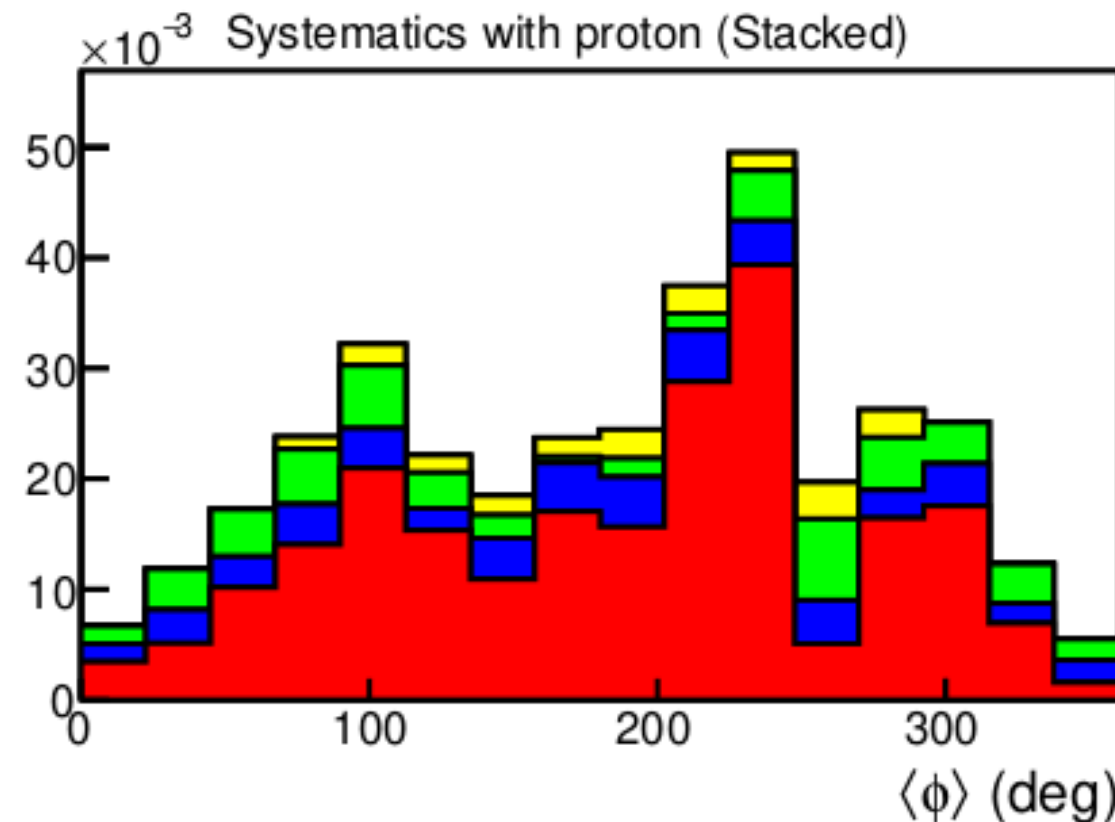
$$\delta A^{cuts} = \frac{\frac{A_{cut}}{\sigma(A_{cut})} - \frac{A}{\sigma(A)}}{\frac{1}{\sigma(A_{cut})} + \frac{1}{\sigma(A)}}$$

**Background subtraction.**

$$\delta A^{Bkg} = \frac{A^{raw} - A^{\pi^0}}{(1 - f)^2} \delta f$$

**Beam polarization**

$$\delta A^{Pol} = A \frac{\delta P}{P}$$



- Smaller systematics when not requiring a proton due to the absence of **exclusivity cuts**
- Total systematic error ranges from 3% to 30% on both torus configurations.
- Proton detection provides better control of the background subtraction systematics
- Exclusivity cuts is the main source of systematics

# 4. BEAM SPIN ASYMMETRY: MERGING DATASETS

BSA measurements were computed separately for each torus configuration, then **merged with a weighted sum**

$$A = \frac{\frac{A_{inb}}{\sigma(A_{inb})^2} + \frac{A_{outb}}{\sigma(A_{outb})^2}}{\frac{1}{\sigma(A_{inb})^2} + \frac{1}{\sigma(A_{outb})^2}}, \quad \sigma(A) = \frac{1}{\sqrt{\frac{1}{\sigma(A_{inb})^2} + \frac{1}{\sigma(A_{outb})^2}}}$$

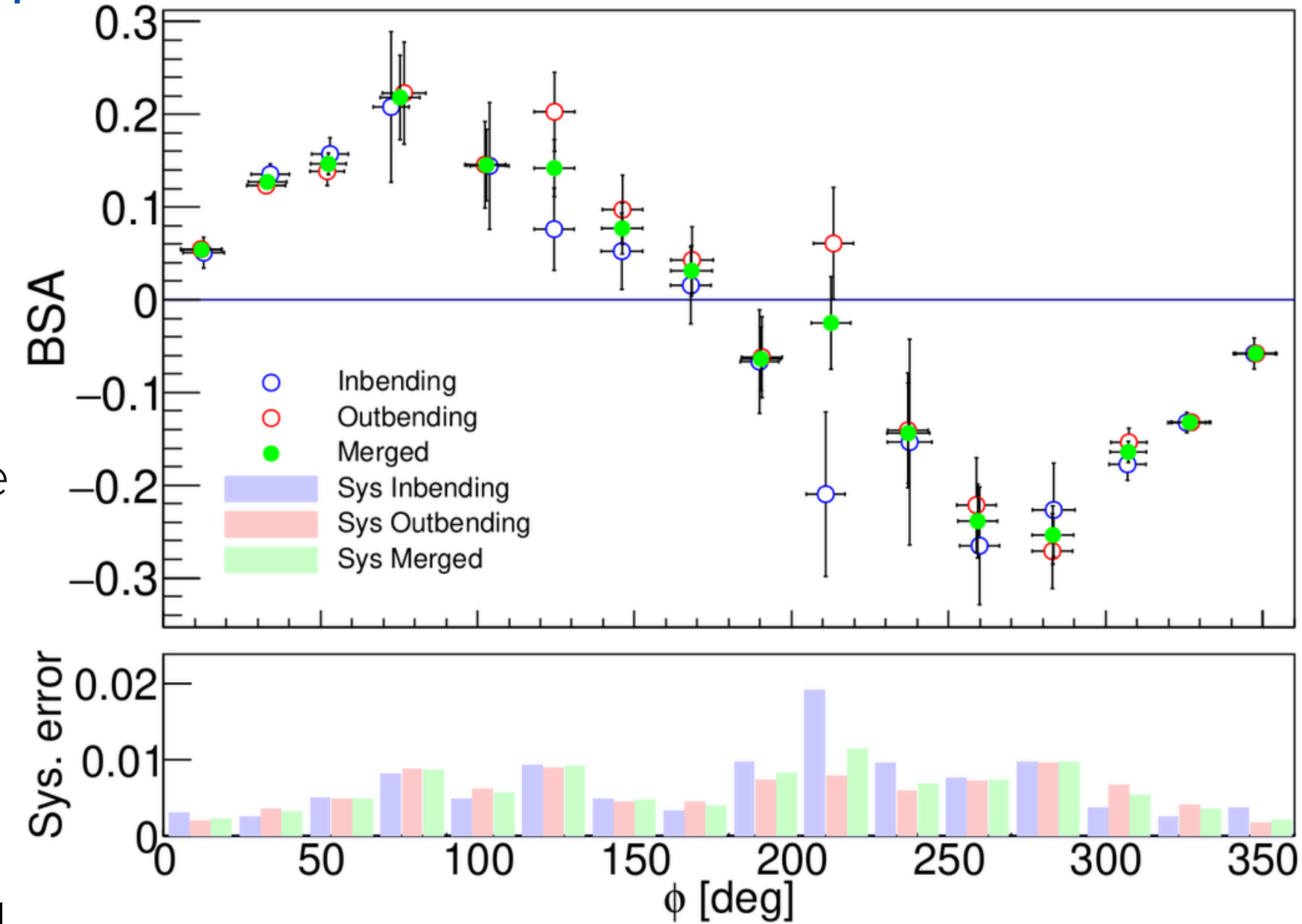
**Merged systematics** are determined by

1. Shifting each configuration BSA with their respective systematics. The computing the weighted average

$$A_{\pm} = \frac{\frac{A_{inb} \pm (\delta A)_{inb}^{cut}}{\sigma(A_{inb})^2} + \frac{A_{outb} \pm (\delta A)_{outb}^{cut}}{\sigma(A_{outb})^2}}{\frac{1}{\sigma(A_{inb})^2} + \frac{1}{\sigma(A_{outb})^2}}$$

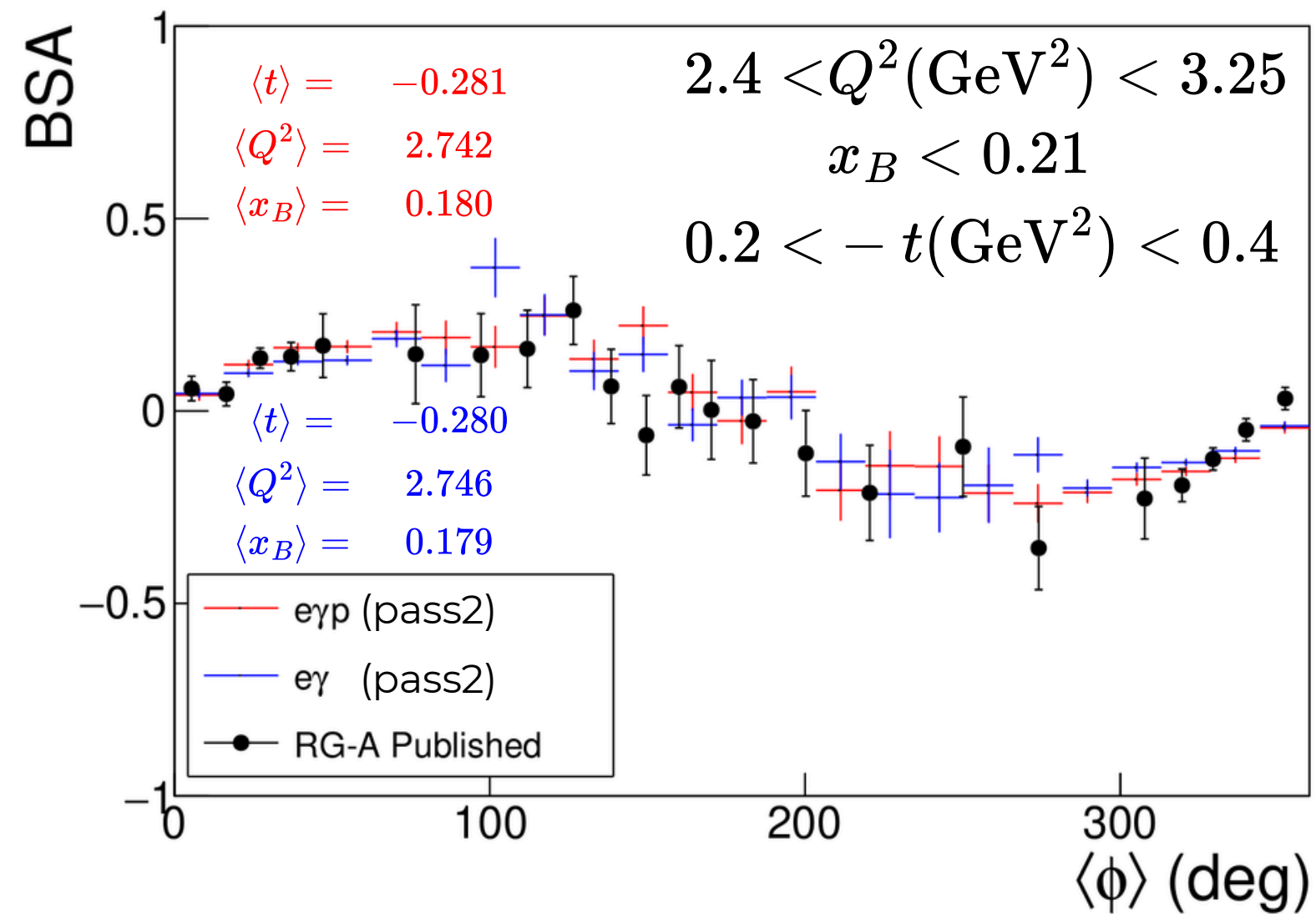
2. Evaluating the quadratic average of the positive- and negative-shifted BSA

$$(\delta A)^{cut} = \sqrt{\frac{(A_+ - A_0)^2 + (A_- - A_0)^2}{2}}$$



$\delta A \rightarrow$  Systematic  
 $\sigma(A) \rightarrow$  Statistical

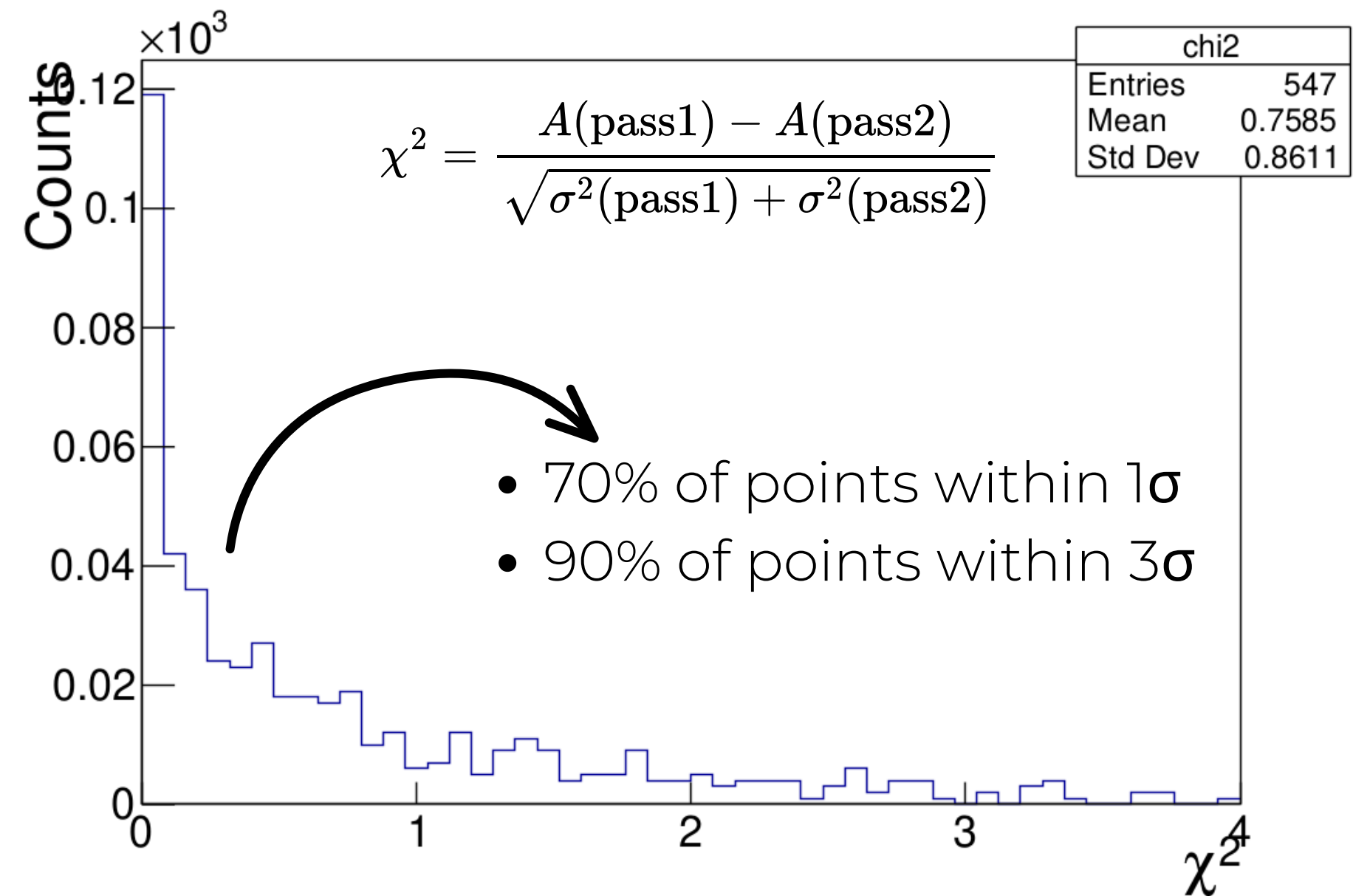
# 5. COMPARISON TO PASST MEASUREMENTS



- Mean kinematics are different point-to-point, and so the BSA
  - The  $\chi^2$  indicates that the two analyses are broadly consistent

Comparison of eyp (pass2) and published (pass1) results

- Using the pass1 binning scheme

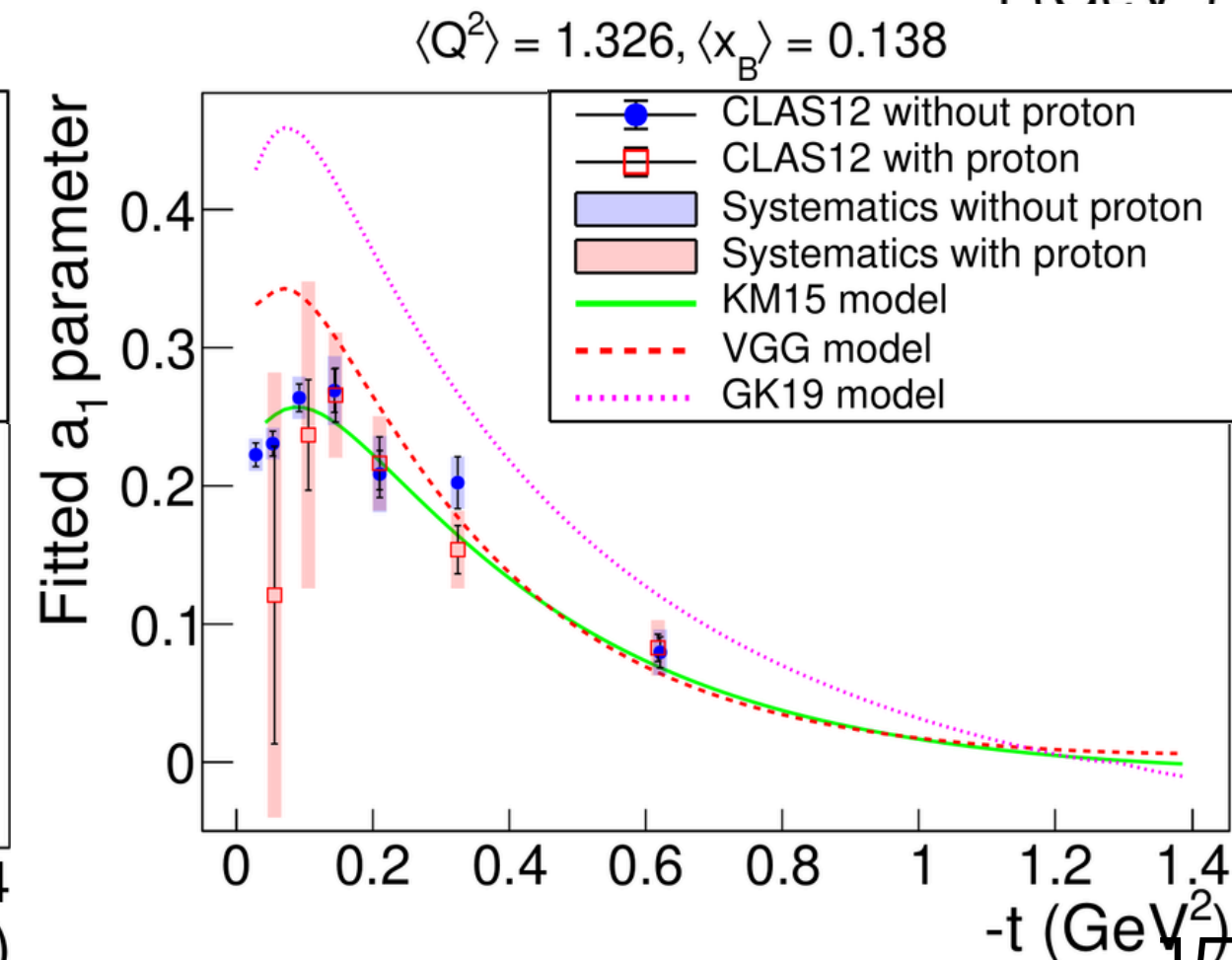
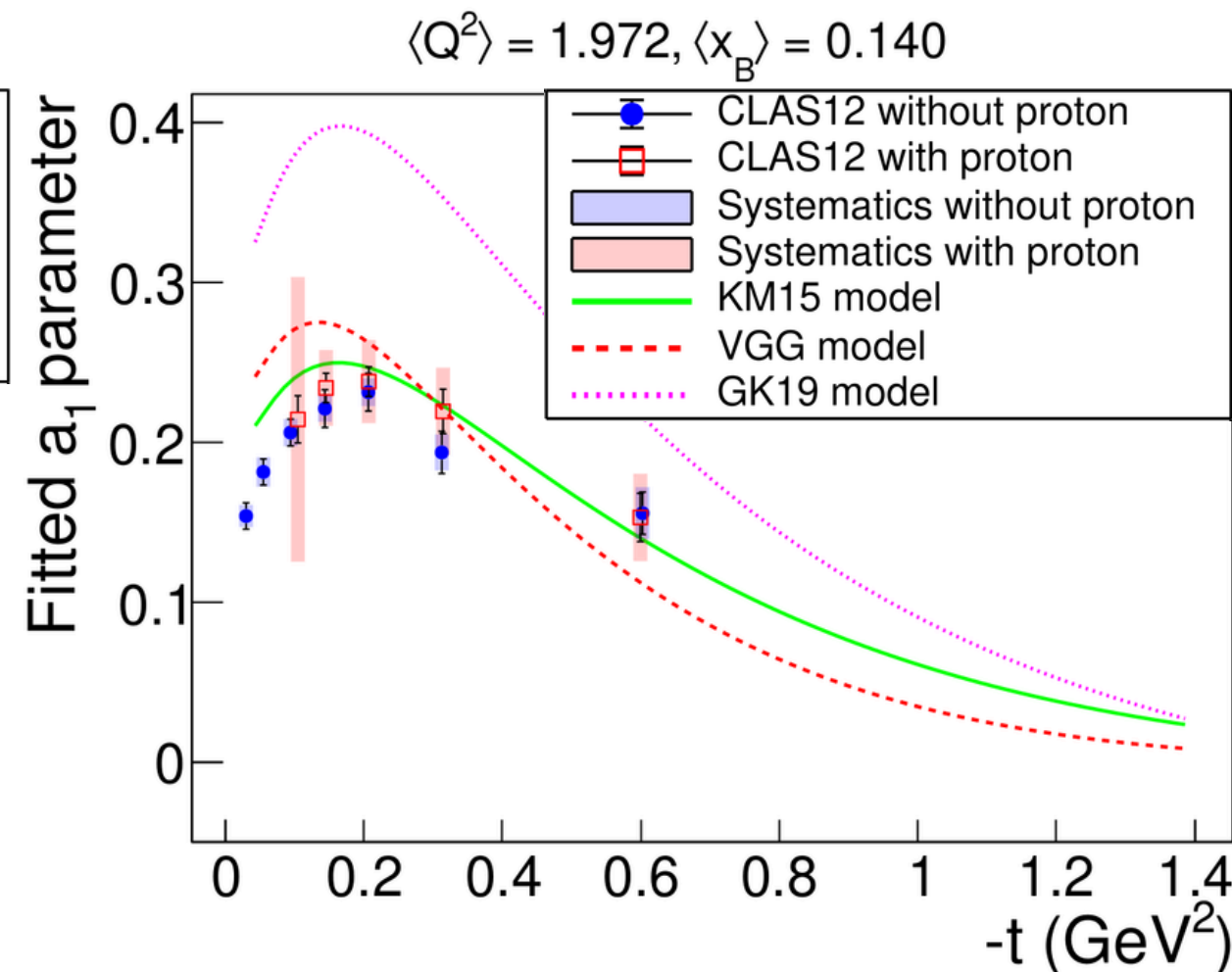
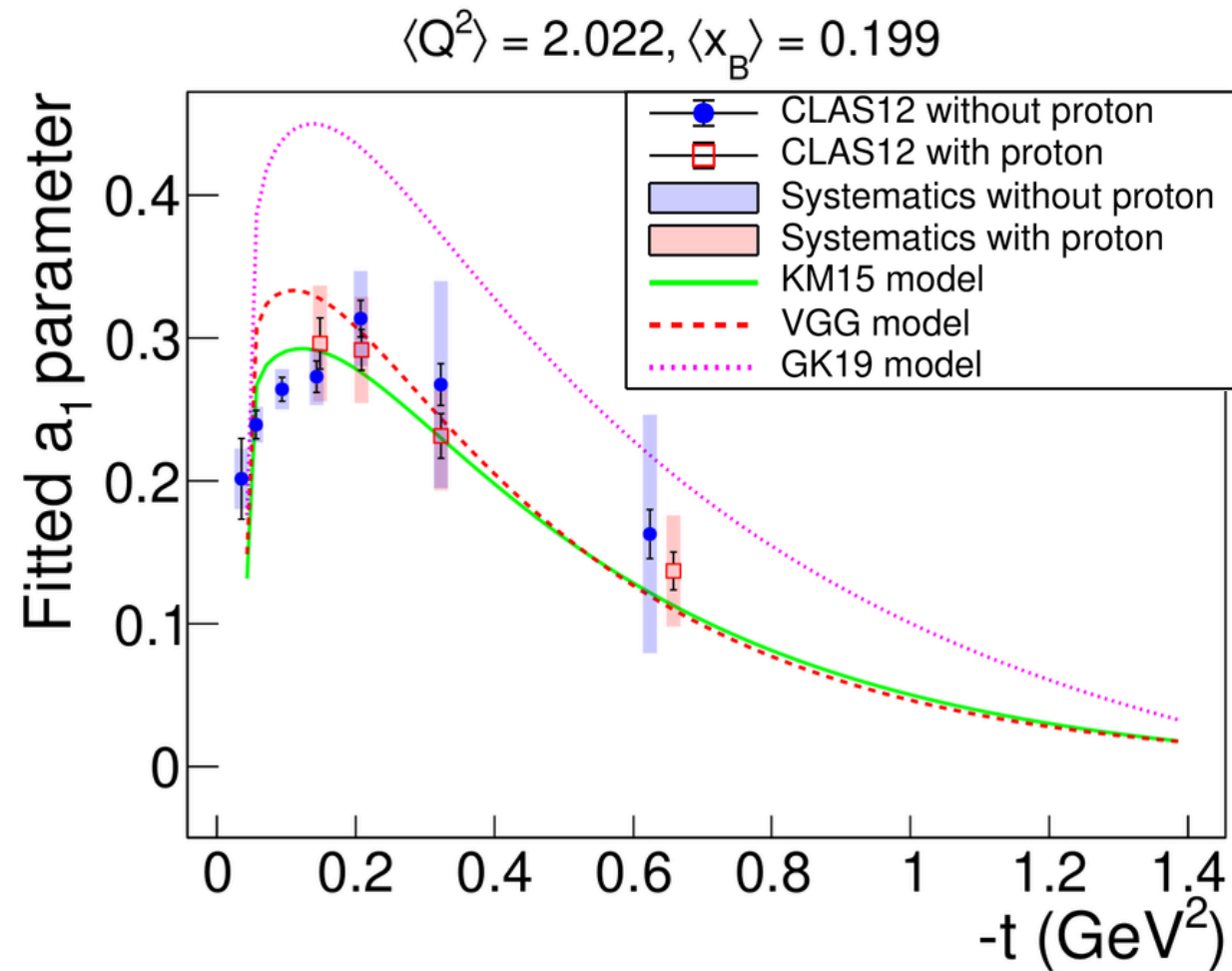
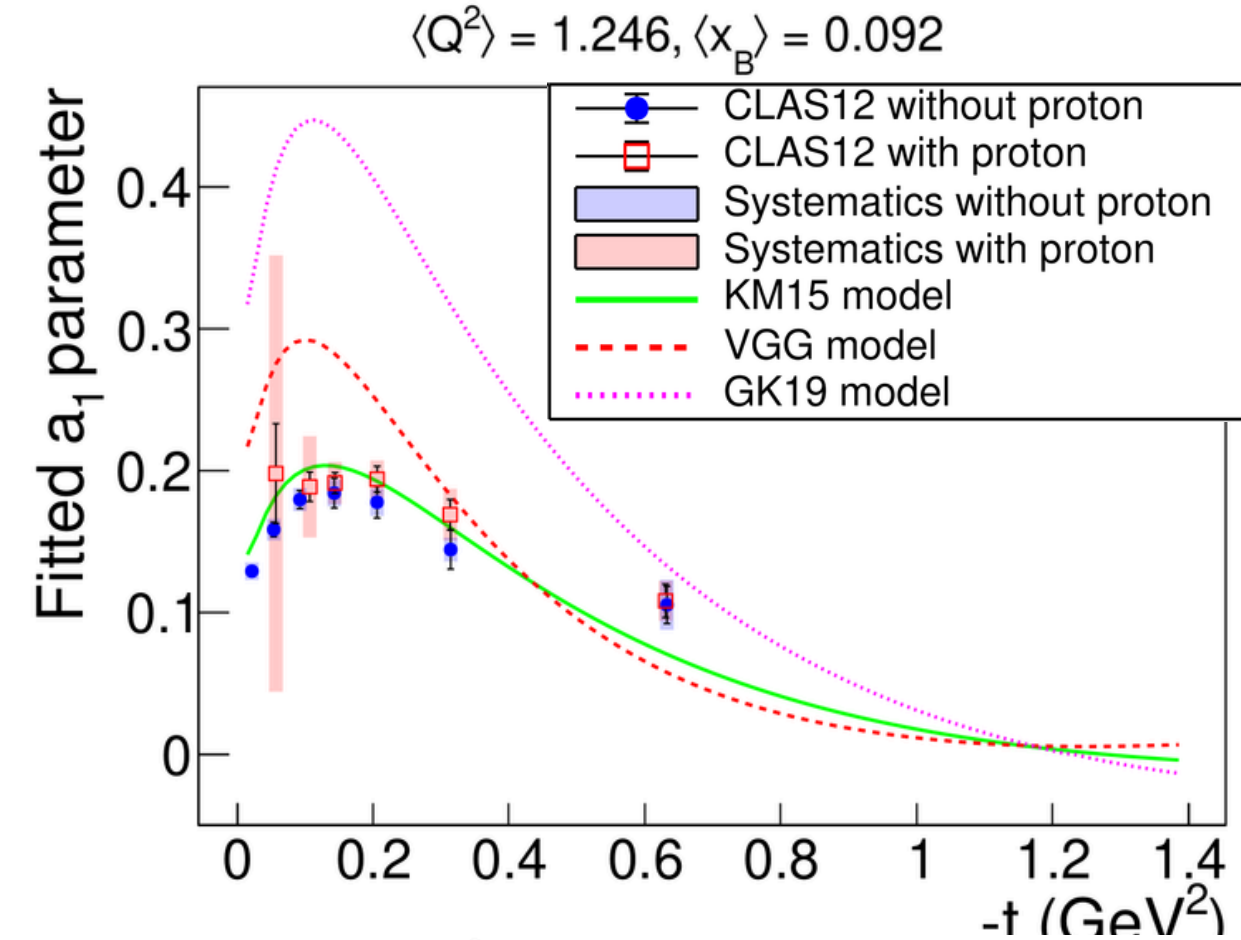


# 6. FITS TO THE BSA

$$A(\phi) \equiv \frac{a_1 \sin(\phi)}{1 + a_2 \cos(\phi)} \quad a_1 \propto \Im \left[ \left( F_1 \mathcal{H} - \frac{t}{4M^2} F_2 \mathcal{E} \right) + \xi (F_1 + F_2) \tilde{\mathcal{H}} \right]$$

Fits to the BSA are displayed as a function of  $-t$  in bins of  $(Q^2, x_B)$

- Agreement of measurements with and without proton
- GK model overestimates the asymmetry
- Large  $|t|$  behavior of VGG and KM15 are similar
  - VGG overestimates the asymmetry at small  $|t|$ .



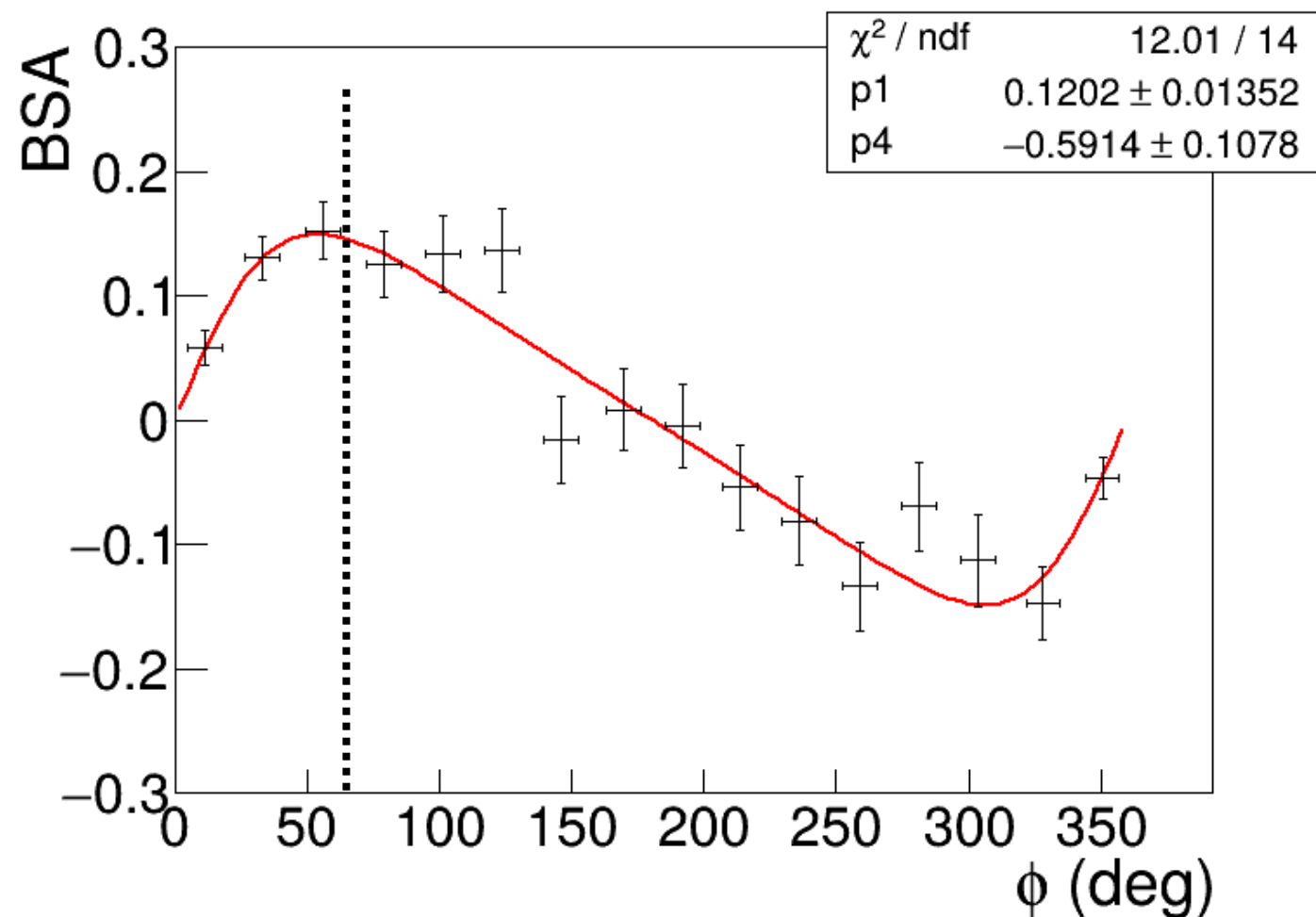
# 6. FITS TO THE BSA

$$A(\phi) \equiv \frac{a_1 \sin(\phi)}{1 + a_2 \cos(\phi)} \quad a_2 \equiv a_2(\Re[CFFs])$$

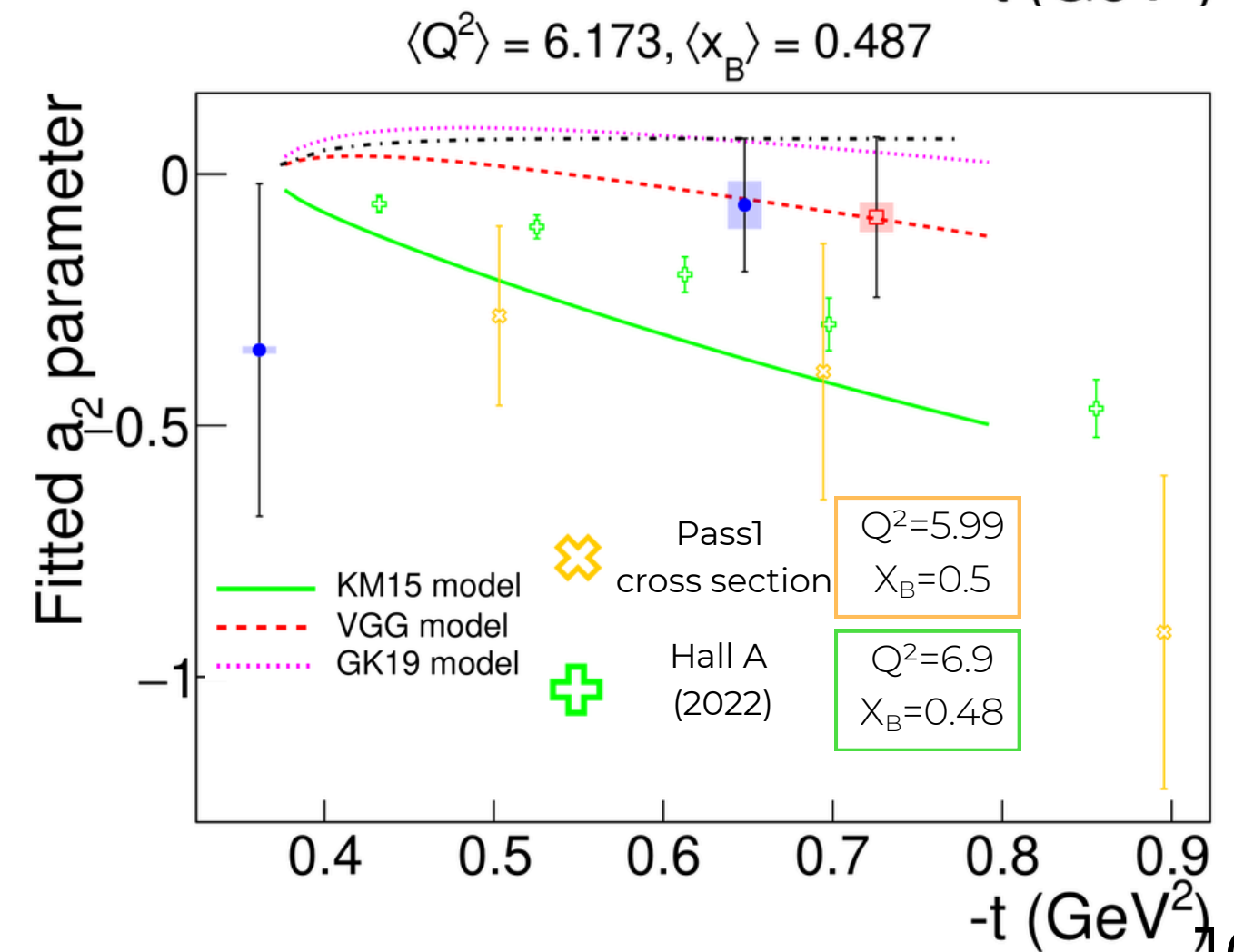
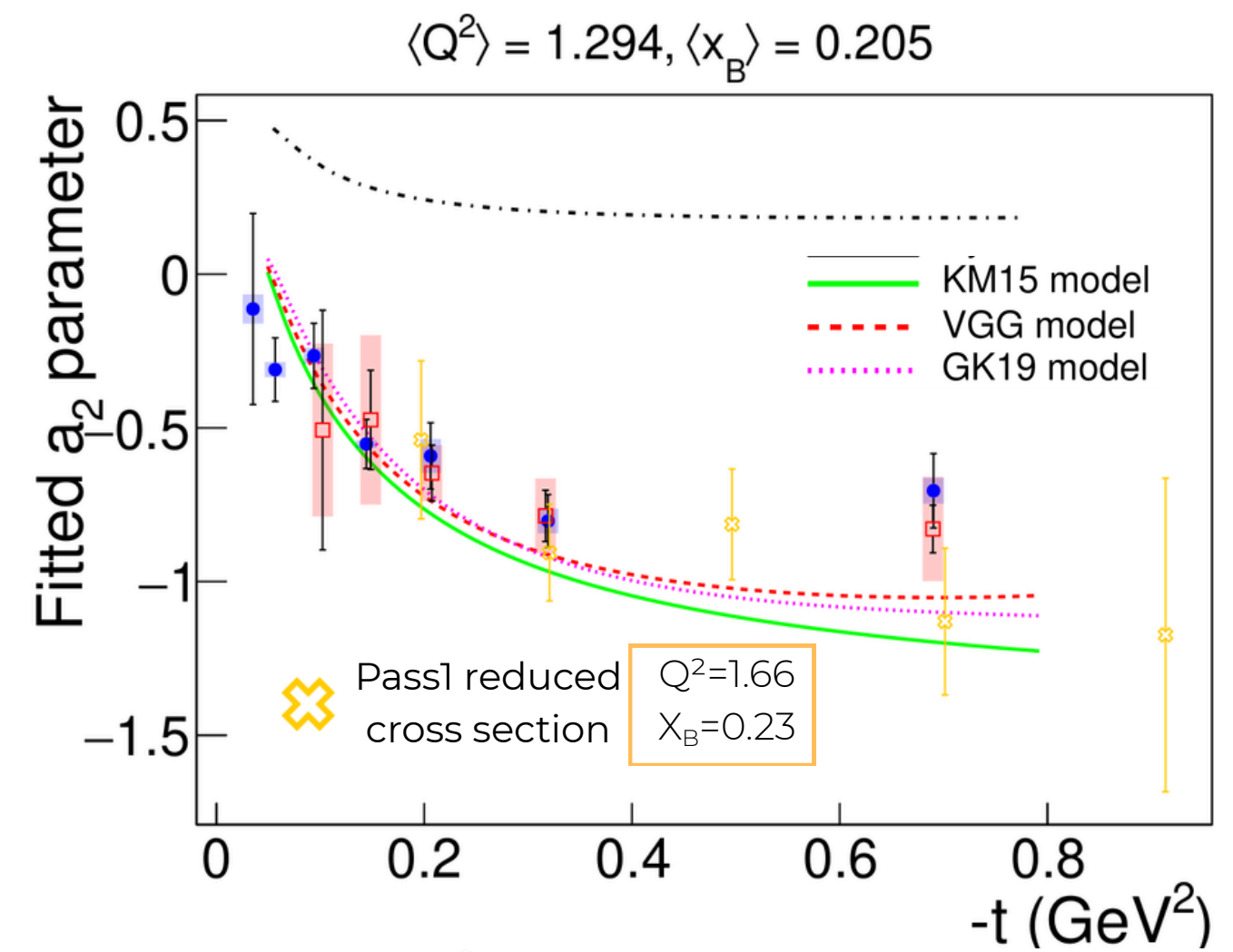
Given the achieved precision on the BSA, constraints on the real part of CFFs can be retrieved

- It shows compatibility with the KM15 model
- It is not BH-dominated and given by:

$$a_2 = \frac{2 \int_0^{2\pi} d\phi \cos(\phi) \mathcal{P}_1 \mathcal{P}_2(\phi) d^5 \sigma_{unp}(\phi)}{\int_0^{2\pi} d\phi \mathcal{P}_1 \mathcal{P}_2(\phi) d^5 \sigma_{unp}(\phi)}$$



- The  $a_2$  parameter shifts the BSA maximum
- $a_2$  is not small w.r.t.  $a_1$
- For scarce statistics, a sinusoidal fit provide misleading results
- It can be contrasted against cross-section measurements

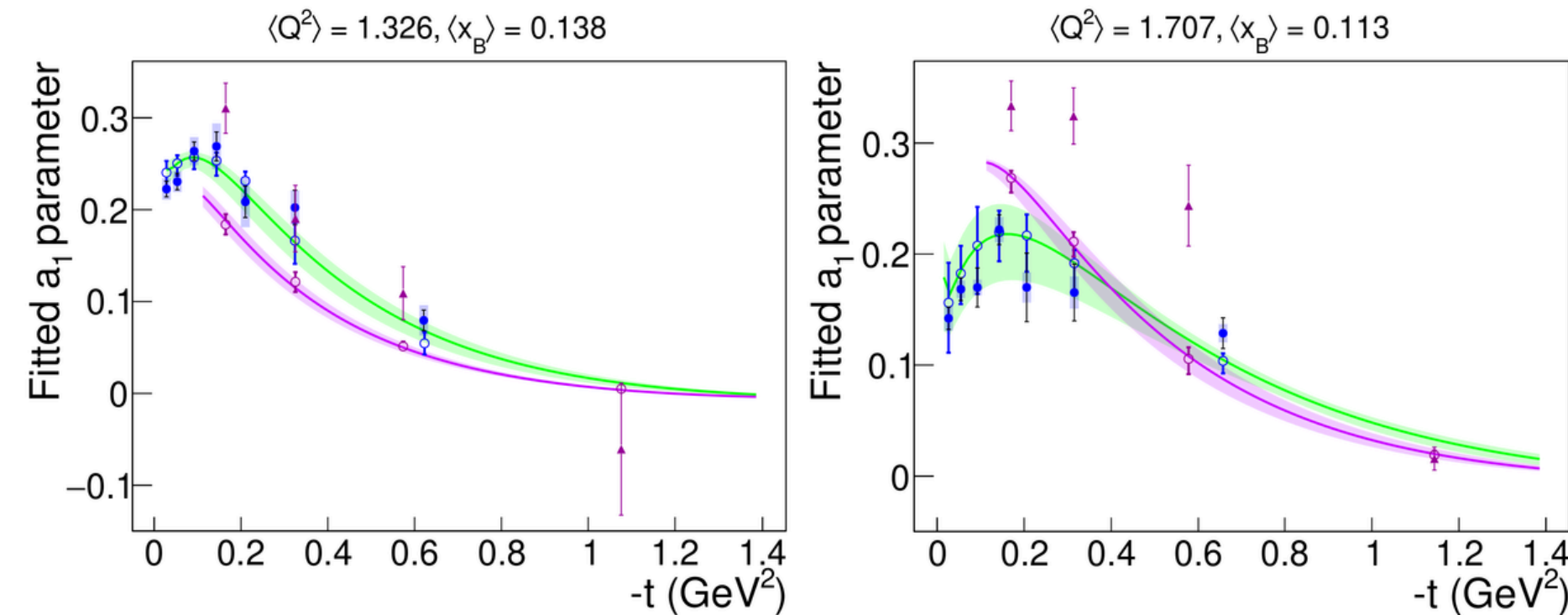
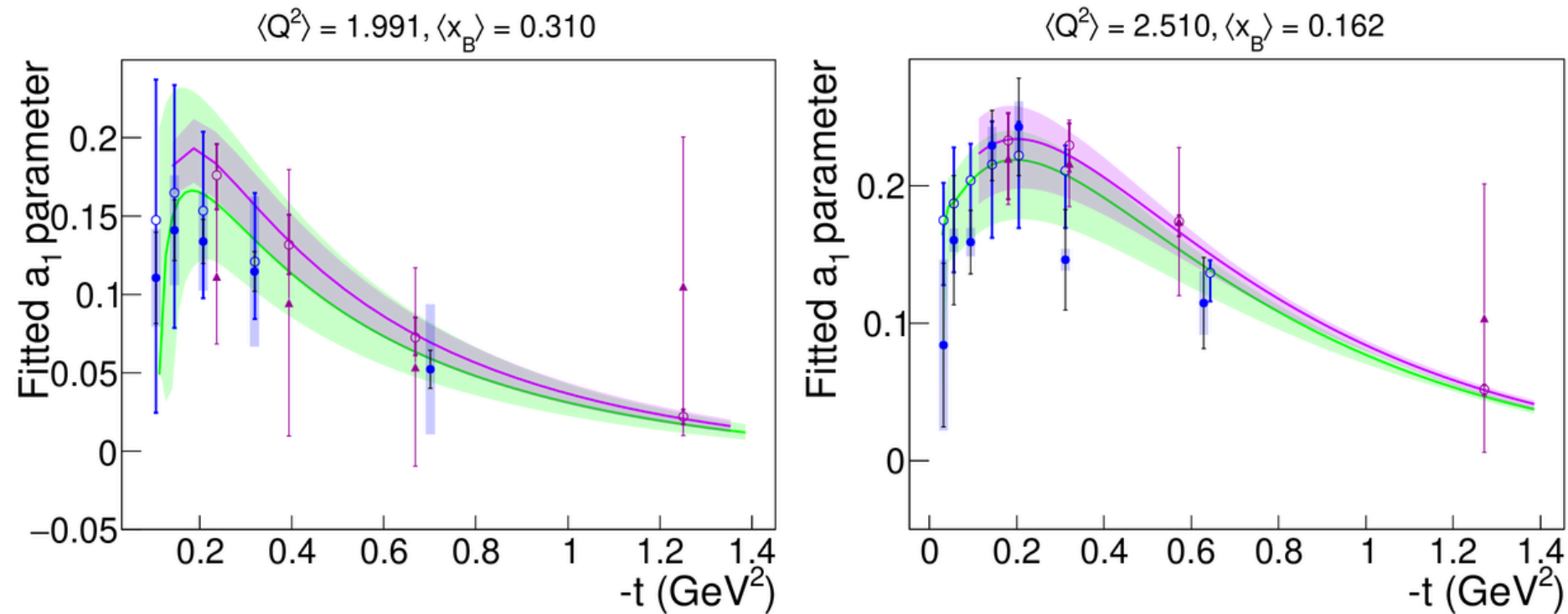


# 6. FITS TO THE PASS1 BSA

To provide a complete picture of the results, fits should be compared to pass1 results

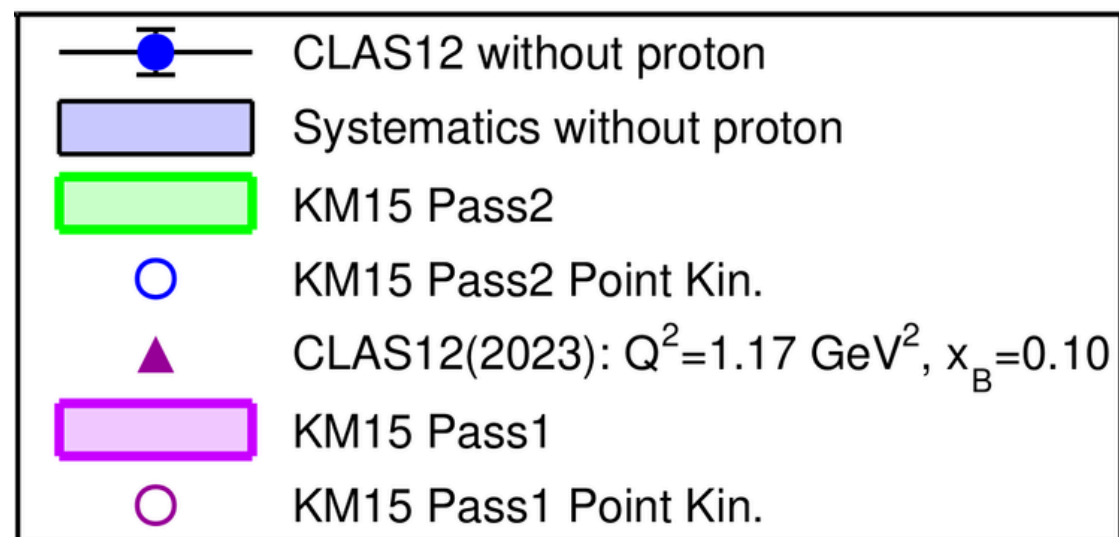
- I performed the fit to the published pass1 data it to the same function

$$A(\phi) \equiv \frac{a_1 \sin(\phi)}{1 + a_2 \cos(\phi)}$$



Most points are compatible within  $1\sigma$ ,

- ...and consistent with the KM15 prediction



Some points are compatible within  $2\sigma$ - $3\sigma$

- Data is not providing a suitable estimate of  $a_2$ , thus biasing the  $a_1$  extraction
- Pass2 result compatible with KM15 prediction, pass1 not so much

# 6. FITS TO THE PASS1 BSA

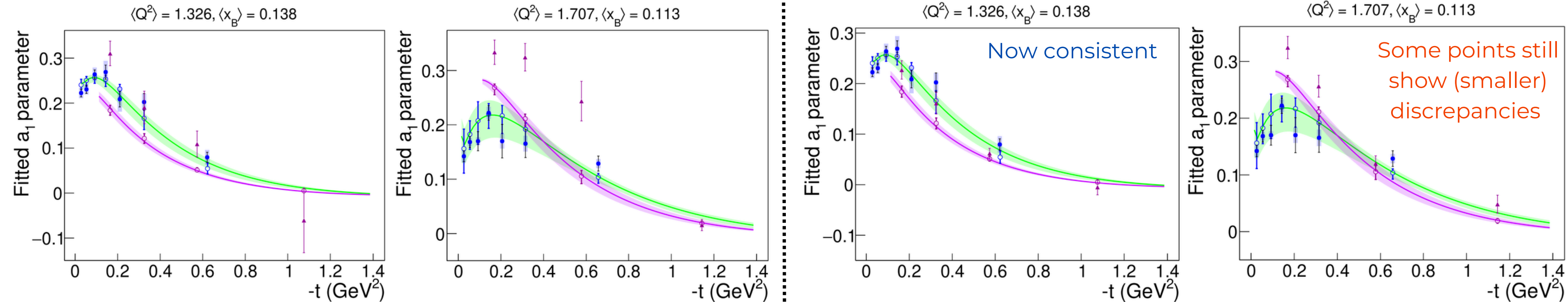
To provide a complete picture of the results, fits should be compared to pass1 results

- I performed the fit to the published pass1 data it to the same function

$$A(\phi) \equiv \frac{a_1 \sin(\phi)}{1 + a_2 \cos(\phi)}$$

$a_1$  and  $a_2$  as free parameters.

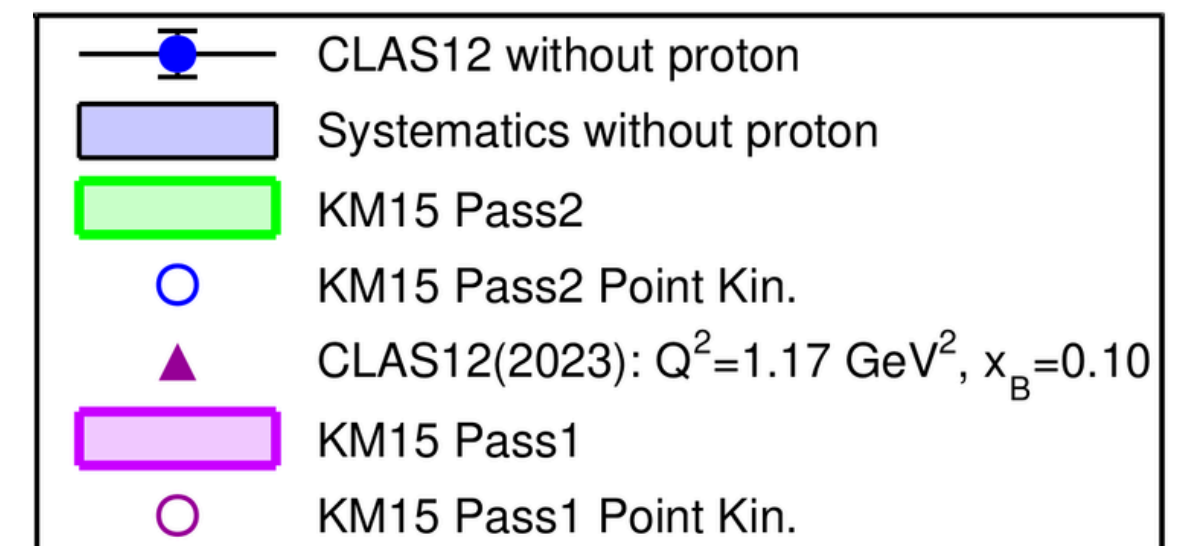
$a_1$  free,  $a_2$  fixed to KM15 prediction



- Given the scarce statistics of the pass1 analysis, fits to the BSA do not provide strong constraints on  $a_2$ , thus biasing the  $a_1$  estimation
- Fixing  $a_2$  to the model prediction might improve certain  $a_1$  estimations.

**REMINDER:** BSA was proven to be consistent.

The fit discrepancy is due to statistical constraints, not to inconsistencies in the data analysis

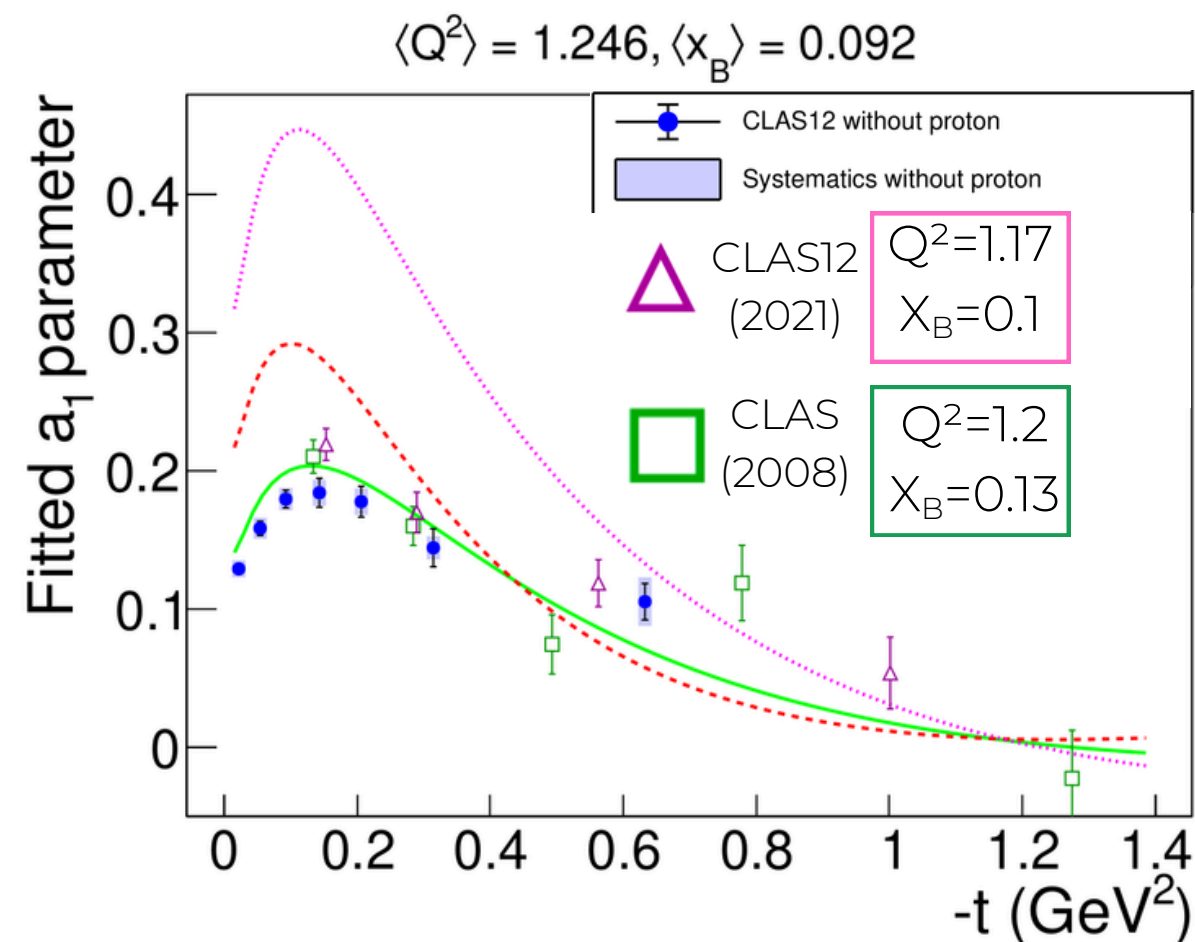


# 7. COMPARISON WITH PREVIOUS EXPERIMENTS

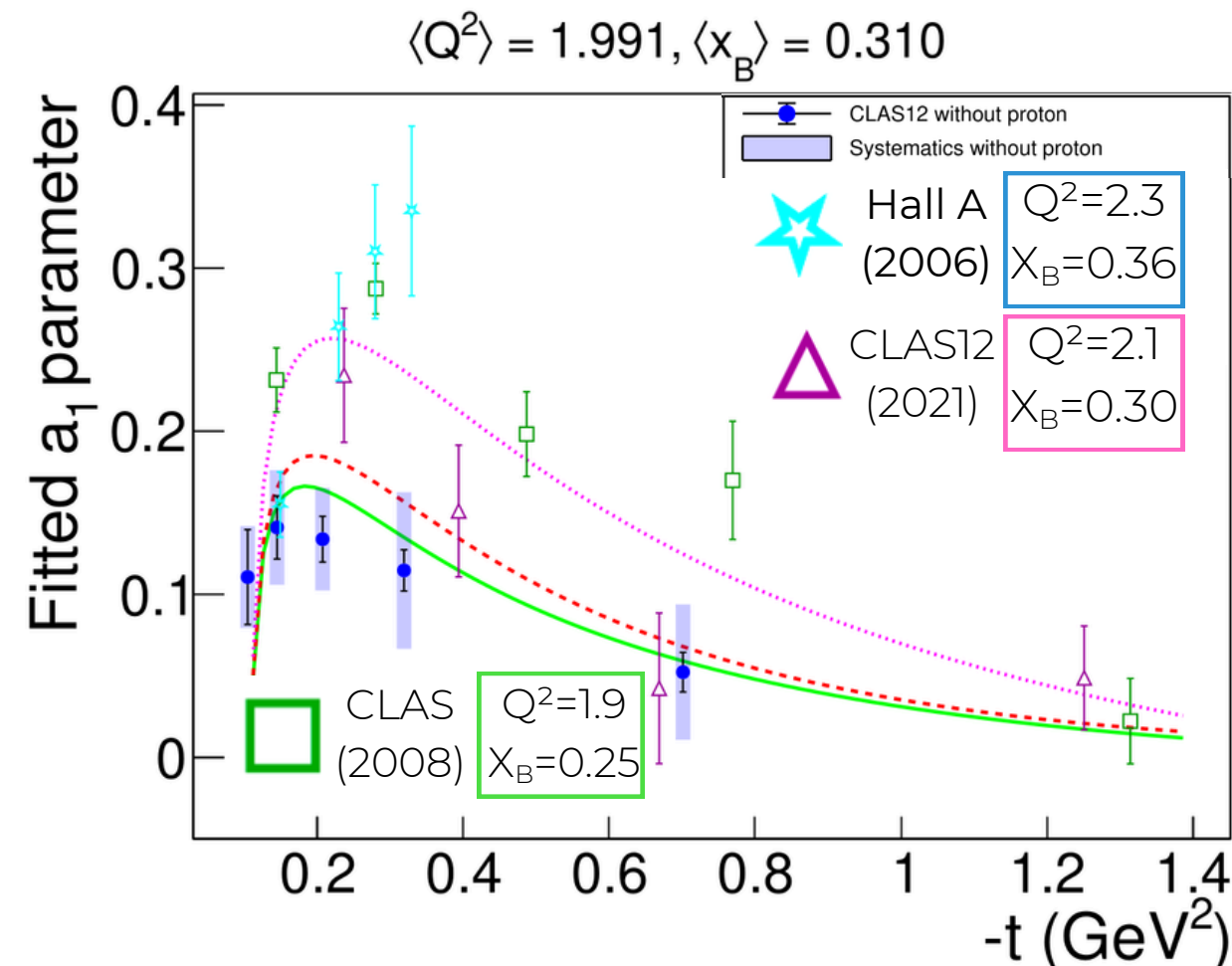
$$A(\phi) \equiv \frac{a_1 \sin(\phi)}{1 + a_2 \cos(\phi)} \quad a_1 \propto \Im \left[ \left( F_1 \mathcal{H} - \frac{t}{4M^2} F_2 \mathcal{E} \right) + \xi(F_1 + F_2) \tilde{\mathcal{H}} \right]$$

We include measurements at close kinematics (yet not identical) from

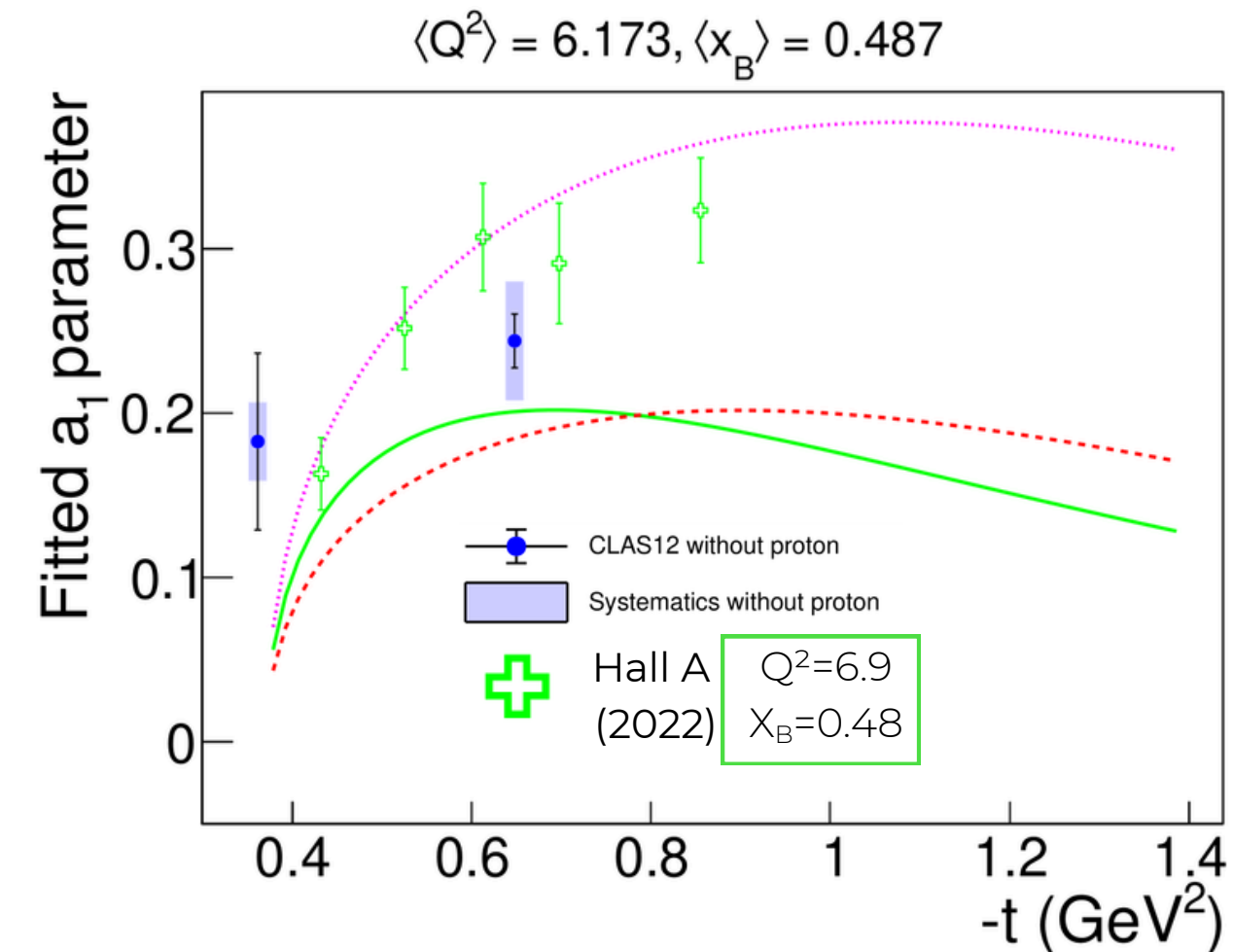
- ★ **Hall A(2006)**: C. Camacho et al., Phys. Rev. Lett. 97.26 (2006), p. 262002.
- **CLAS(2008)**: F. X. Girod et al., Phys. Rev. Lett. 100.16 (2008), p. 162002.
- ⊕ **Hall A(2022)**: F. Georges et al., Phys. Rev. Lett. 128.25 (2022): 252002.
- △ **CLAS12(2021)**: G. Christiaens, et al. Phys. Rev. Lett. 130 (2023) 211902.



At similar kinematics, results are consistent with CLAS measurements



A fair comparison cannot be performed due to **different kinematics**



At large  $x_B$ , Hall A precision is unmatched

# 8. SUMMARY

---

In brief, I have presented:

- **A DVCS event selection strategy based on Boosted Decision Trees.**
  - Provides good control of background sources. Leftover background subtraction needed
  - Optimizes the signal yield
- **A method for selecting DVCS events without requiring proton detection**
  - Boosts statistics
  - Access to a larger phase space (unique access to the small -t region)
- **BSA measurements, with and without proton detection**
  - $ey(p)$  measurements have smaller systematic errors
  - Results were shown to be consistent with the published pass1 results
- **Fits to the BSA**
  - Results show a fair agreement with the KM15 model predictions
  - Precise extractions of  $a_1$  were presented
    - Data allows us to constrain the  $a_2$  parameter as well.
  - Reduced pass 1 statistics demands a model-driven fit to reconcile with pass2 measurements
  - Consistent picture with the measurements of previous experiments
    - Not a fair comparison due to the different mean kinematics in several  $(Q^2, x_B)$  bins.
- **Article draft in ad-hoc review (PRL). First round of comments has been received.**

$$A(\phi) \equiv \frac{a_1 \sin(\phi)}{1 + a_2 \cos(\phi)}$$

THANKS

---